# *Time-frequency analysis of chaotic systems*

T. Uzer
Georgia Institute of Technology

Collaboration: C. Chandre (Univ. of Marseille)
S. Wiggins (Bristol)

antoine 95

RAPID COMMUNICATIONS

PHYSICAL REVIEW A VOLUME 51, NUMBER 3 MARCH 1995

# Time profile of harmonics generated by a single atom in a strong electromagnetic field

Philippe Antoine and Bernard Piraux
*Institut de Physique, Université Catholique de Louvain, 2, Chemin du Cyclotron, B1348 Louvain-La-Neuve, Belgium*

Alfred Maquet
*Laboratoire de Chimie Physique—Matière et Rayonnement, Université Pierre et Marie Curie, 11, rue Pierre et Marie Curie, 75231 Paris Cedex 05, France*

(Received 7 September 1994)

We show that the time profile of the harmonics emitted by a single atom exposed to a strong electromagnetic field may be obtained through a wavelet or a Gabor analysis of the acceleration of the atomic dipole. This analysis is extremely sensitive to the details of the dynamics and sheds some light on the competition between the atomic excitation or ionization processes and photon emission. For illustration we study the interaction of atomic hydrogen with an intense laser pulse.

PACS number(s): 32.80.Rm, 42.50.Hz

It is now well established that an atom exposed to an intense laser pulse can emit high order harmonics of the driving force. At high field intensity and for a wide range of frequencies, all harmonic spectra share the same qualitative behavior characterized by the existence of a plateau. Until now, the main effort has focused on the study of the overall behavior of the harmonics spectra at high intensity and low frequency, where most of the experiments have been performed. It has been surmised by means of a semiclassical model that in this regime, the highest harmonics of the plateau are produced by electrons which, after tunneling out, return to the vicinity of the ion with a very high kinetic energy [1].

$$i\frac{\partial}{\partial t}\Psi(\mathbf{r},t)=[H_0+\mathbf{A}(t)\cdot\mathbf{p}]\Psi(\mathbf{r},t), \tag{1}$$

where $H_0$ is the atomic Hamiltonian and $\mathbf{A}(t)$ the vector potential associated with the field:

$$\mathbf{A}(t)=A_0 f(t)\sin(\omega t)\mathbf{e}_z \ ; \tag{2}$$

$A_0$ is the amplitude of the potential, $\mathbf{e}_z$ is the unit vector along the $z$ axis, $\omega$ is the frequency of the laser field, and $f(t)$ is a slowly varying envelope assumed here to be Gaussian. The numerical procedure is the following: we first expand the wave function $\Psi(\mathbf{r},t)$ of the system in a basis of

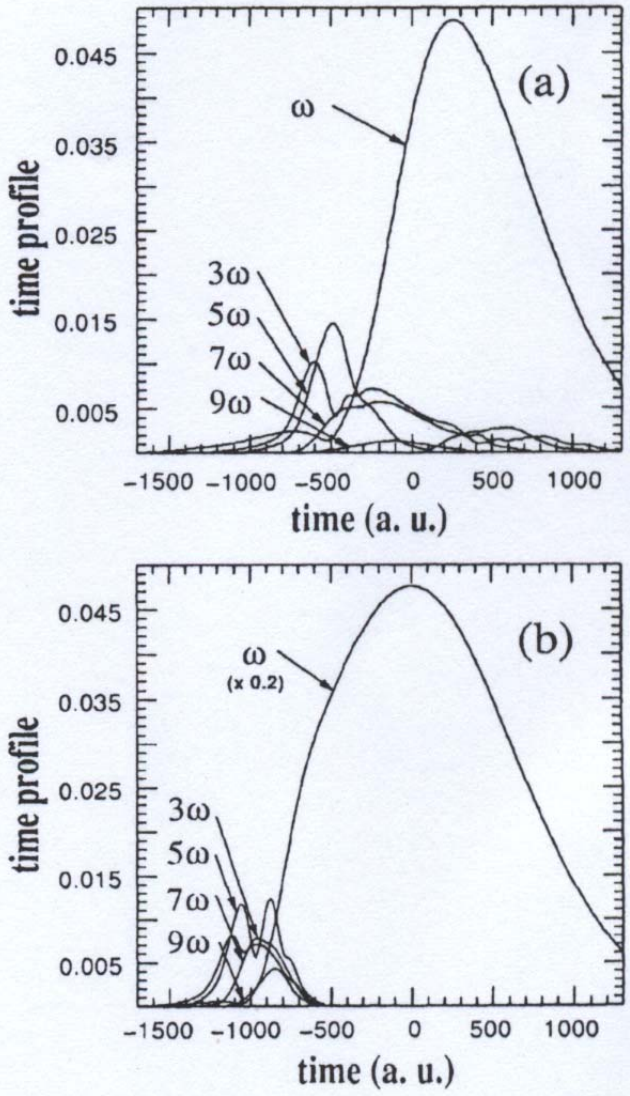


FIG. 2. Time profile [given by the coefficient $\tilde{a}(\alpha,\beta)$] of the odd harmonics (1–9) for the same cases as in Fig. 1. (a) $I_0=2\times10^{14}$ W/cm$^2$ and (b) $I_0=2\times10^{15}$ W/cm$^2$.

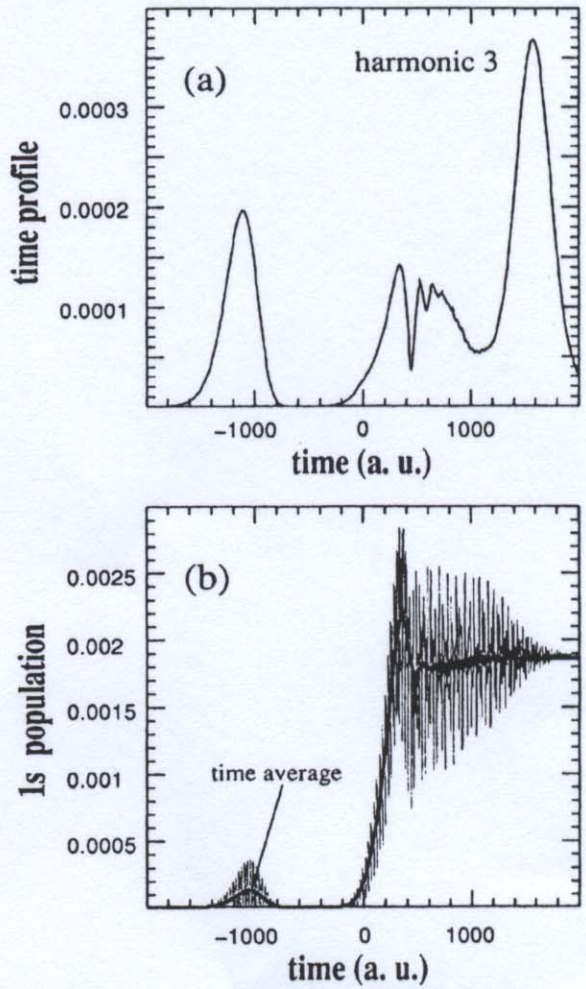


FIG. 4. (a) Time profile of the third harmonic emitted by atomic hydrogen initially in its $2s$ state and exposed to a Gaussian pulse of $I_0=2\times10^{14}$ W/cm$^2$, FWHM=20 optical cycles, and laser frequency $\omega=0.118$ a.u. (b) $1s$ population (i.e., the projection of the full wave function on the bare $1s$ state of atomic hydrogen) as a function of time in atomic units for the same case as in (a). The thick line represents the time average of the $1s$ population.

INSTITUTE OF PHYSICS PUBLISHING JOURNAL OF PHYSICS B: ATOMIC, MOLECULAR AND OPTICAL PHYSICS

J. Phys. B: At. Mol. Opt. Phys. **38** (2005) L339–L346 doi:10.1088/0953-4075/38/20/L02

**LETTER TO THE EDITOR**

# Asymmetry in the harmonic generation from nonsymmetric molecules

**G Lagmago Kamta[1], A D Bandrauk[1] and P B Corkum[2]**

[1] Département de Chimie, Université de Sherbrooke, Sherbrooke, Québec, J1K 2R1, Canada
[2] National Research Council of Canada, Ottawa, Ontario, K1A 0R6, Canada

E-mail: gerard.lagmago.kamta@usherbrooke.ca

Received 13 July 2005, in final form 12 September 2005
Published 27 September 2005
Online at stacks.iop.org/JPhysB/38/L339

**Abstract**

We report a calculation of the harmonic emission from a one-electron heteronuclear nonsymmetric molecule ($HeH^{2+}$) interacting with a few-cycle laser pulse linearly polarized along the molecular axis. We find that a 180° rotation of the molecule (or equivalently a 180° change in the carrier-envelope phase) leads to substantial changes in the harmonic emission of the molecule. Phase-dependent plateaux and cutoffs appear in the harmonic spectrum as a consequence of the phase-dependent electric field of few-cycle pulses. Asymmetries in the intensity of harmonics result from the phase dependence of ionization rates in nonsymmetric molecules, and from the fact that depending on the molecular orientation, the ionized electron wavepacket can be Coulomb focused as it visits the proton twice before the recollision leading to harmonic generation.

When driven by intense laser fields, atomic and molecular systems emit radiation at frequencies multiple of that of the driving field. This nonlinear process, known as harmonic generation (HG), has widely been studied theoretically and experimentally [1, 2]. High-order harmonic generation (HOHG) agrees with a semiclassical interpretation (the so-called 'three step model') that the electron first tunnels through a potential barrier, is accelerated by the laser field and then driven back for a recollision with the core, upon which harmonic radiation is emitted [3, 4]. A typical harmonic spectrum from an atom consists of odd harmonics only, with rapidly decreasing intensities for the first few harmonics, followed by a region of almost constant harmonic intensities (the plateau), and ends with a cutoff which determines the maximum harmonic in the spectrum [3–5]. The spectrum from symmetric (homonuclear) molecules is similar to that of atoms, except that depending on their orientation with respect to the laser polarization, extrema may appear, due to destructive or constructive interferences of contributions originating from each nucleus [6–10].

The vector potential of a linearly polarized laser pulse can be written in the dipole approximation as

$$\mathbf{A}(t, \phi) = A_0 f(t) \sin(\omega_0 t + \phi)\mathbf{e}_z, \tag{1}$$

0953-4075/05/200339+08$30.00 

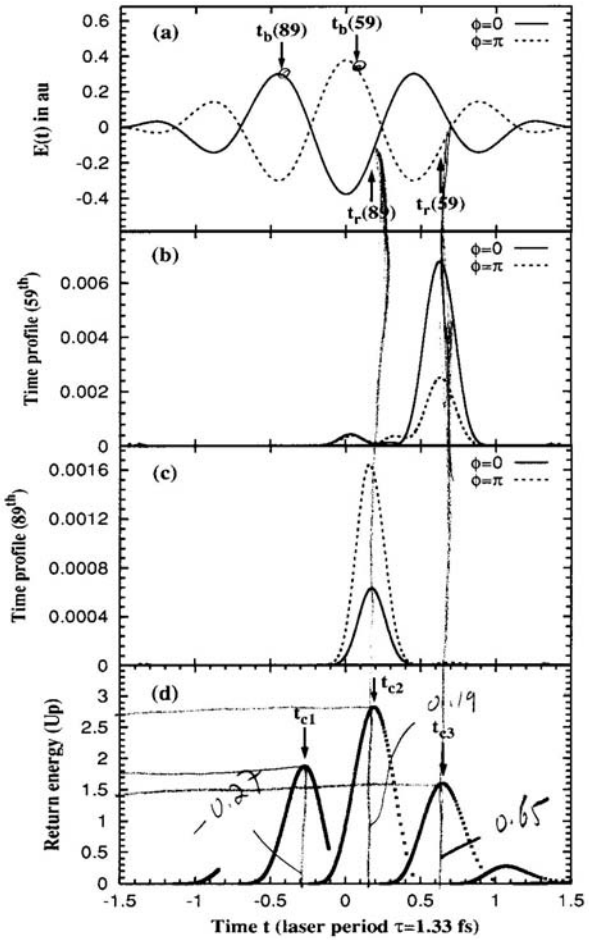


**Figure 2.** (a) The electric field $E(t,\phi) = \frac{d}{dt}A(t)$, for absolute phases $\phi = 0$ and $\phi = \pi$. (b) Time profile (arb. units) of the 59-th harmonic of $HeH^{2+}$ for the absolute phases $\phi = 0$ and $\phi = \pi$. (c) Same as (b) for the 89-th harmonic. (d) Classical kinetic energy of the electron at its first return to the molecular core versus its return time. The internuclear distance and laser parameters are the same as in figure 1.

the time $t_r(59)$. This means that for both $\phi = 0$ and $\phi = \pi$, high-order harmonics below the first cutoff are emitted predominantly at time $t_r(59)$. The profile of the 89-th harmonic in figure 2(c) also shows a single prominent peak, which is centred at time $t_r(89) = 0.17\tau$. Here again, increasing the FWHM of the window function and placing its centre at the local maxima between the two cutoffs still leads to a prominent peak at time $t_r(89)$. Thus, harmonics between the first and second cutoffs are predominantly emitted at about time $t_r(89)$.

For the internuclear distance $R = 15$ au, more than 99% of the electron cloud in the ground state of $HeH^{2+}$ is localized on the $He^{2+}$ nucleus (i.e., the wavefunction is negligible in the vicinity of the proton $H^+$), so that in the perspective of the 'three step model' of HOHG the

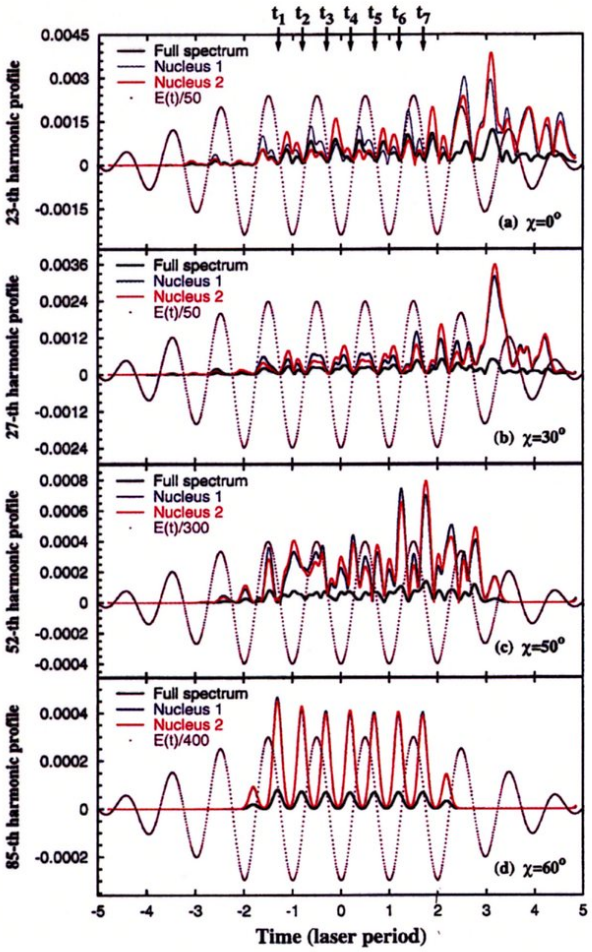


FIG. 10. (Color) Time profiles (in arb. units) for harmonic orders in the vicinity of interference minima in the spectra of $H_2^+$ (see Fig. 8) for the peak intensity $I=5\times10^{14}$ W/cm$^2$. The following are plotted for orientation angles $\chi$ shown: the scaled electric field (magenta dots), the time profiles of the full harmonic spectrum of $H_2^+$ with interferences included (black lines), the time profiles of harmonic spectra originating from the nucleus 1 (blue lines) and from the nucleus 2 (red lines). The instants $t_j$ ($j=1-7$) are the classical times of first electron return as described in Fig. 9.

However, photon emission for harmonics at the interference minima for other orientation angles [see Figs. 10(a)–10(c)] show the occurrence of harmonic emission at times that do not correspond to short trajectories. The semiclassical recollision model predicts that at lower energies, i.e., lower harmonics, two recollision trajectories should dominate, coalescing into one single trajectory at the maximum cutoff energy [46,47]. Thus, at lower energies, one extra trajectory, called the long trajectory, is expected to return to the molecular core at the peak of the electric field. This extra trajectory has been recently characterized [45]. Figure 10 illustrates quantitatively this semiclassical prediction, as the profiles indicate harmonic emission (recollisions) occurring near the maxima (minima) and the zeros of the electric field for harmonics well below the cutoff [see Figs. 10(a)–10(c)]. Note that for double trajectories (low-order harmonics) and single trajectories (high-order harmonics), efficient destructive interference is seen to occur, reflecting the fact that photon emission amplitudes at each nucleus are out of phase with each other. Next, we examine the theoretical formulations that allow to elucidate these multicenter interference phenomena, which occur only in molecules and which have already been predicted to occur in molecular ATI spectra [12].

## VII. ACCELERATION VERSUS DIPOLE PHOTON EMISSION

It has been shown that the correct evaluation of the harmonic spectrum is to proceed via the Fourier transform $\mathbf{A}(\omega)$

## Intramolecular relaxation rates

*statistical theories ( RRKM theory ) : assumption of uniformity of phase space*

*predicted relaxation rate:* $\tau_\lambda = \frac{1}{\lambda} \approx 0.17$ ps

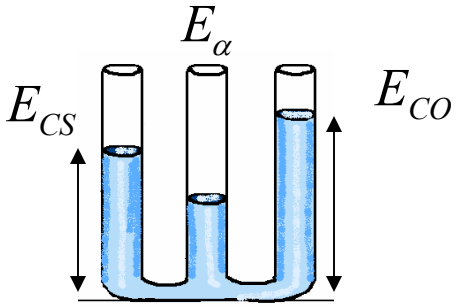


**normal mode analysis**

$$\begin{cases} E = E_{CO} + E_{CS} + E_{bend} \\ E_i = \frac{p_i^2}{2\mu_i} + \omega_{0i}^2 q_i^2 \end{cases}$$

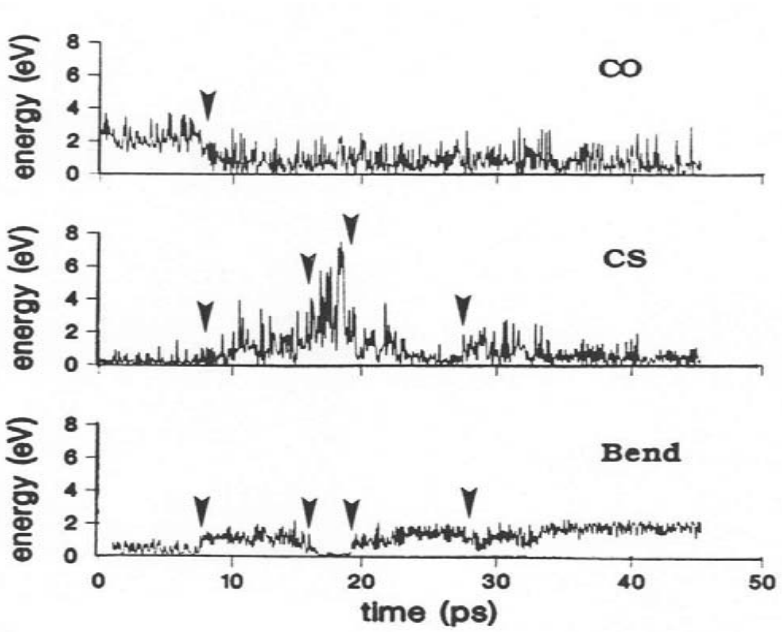


*observed relaxation rate:* $\tau > 10$ ps

*Reference:* D. Carter, *et al, J. Chem. Phys,* **77,** 4208, (1982)

## *planar carbonyl sulfide (OCS)*

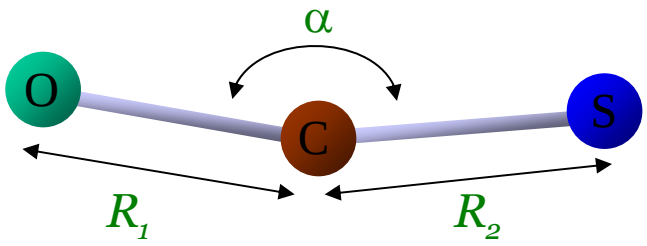


> 3 modes: OC stretch, CS stretch, OCS bend

$$H = T(P_1, P_2, P_\alpha, R_1, R_2, \alpha) + \sum_{i=1}^{3} V_m(R_i) + AP(R_1, R_2, R_3) \prod_{i=1}^{3} V_I(R_i)$$

kinetic energy — Morse — quartic polynomial — Sorbie-Murrell potential

$$T = \frac{\mu_1}{2} P_1^{\,2} + \frac{\mu_2}{2} P_2^{\,2} + \mu_3 P_1 P_2 \cos\alpha + P_\alpha^{\,2} \left( \frac{\mu_1}{2R_1^{\,2}} + \frac{\mu_2}{2R_2^{\,2}} - \frac{\mu_3 \cos\alpha}{R_1 R_2} \right) - \frac{\mu_3 P_1 P_\alpha \sin\alpha}{R_2} - \frac{\mu_3 P_2 P_\alpha \sin\alpha}{R_1}$$

$$V_m(R_i) = D_i \left( 1 - e^{-\beta_i (R_i - R_i^{\,0})} \right)^2$$

$$V_I(R_i) = 1 - \tanh\left( \gamma_i (R_i - \tilde{R}_i) \right)$$

$$P(R_1, R_2, R_3) = 1 + \sum_i c_i R_i + \sum_{i,j} c_{ij} R_i R_j + \sum_{i,j,k} c_{ijk} R_i R_j R_k + \sum_{i,j,k,l} c_{ijkl} R_i R_j R_k R_l$$

$$R_3 = \|OS\| = \sqrt{R_1^{\,2} + R_2^{\,2} - 2R_1 R_2 \cos\alpha}$$


References:

Carter, Brumer, *J. Chem. Phys.* **77** (1982), 4208
Foord, Smith, Whiffen, *Mol. Phys.* **29** (1975), 1685
Bunker, *J. Chem. Phys.* **37** (1962), 393

## Analysis of trajectories of Hamiltonian systems $H(\boldsymbol{p},\boldsymbol{q};t)$

$$\begin{cases} \dfrac{\mathrm{d}\boldsymbol{p}}{\mathrm{d}t} = -\dfrac{\partial H}{\partial \boldsymbol{q}} \\ \dfrac{\mathrm{d}\boldsymbol{q}}{\mathrm{d}t} = +\dfrac{\partial H}{\partial \boldsymbol{p}} \end{cases} \Rightarrow \left\{\boldsymbol{p}(t),\boldsymbol{q}(t)\right\}_{t\in[0,T]} \Rightarrow \left\{\boldsymbol{p}(t_i),\boldsymbol{q}(t_i)\right\}_{i=1,\ldots,N}$$

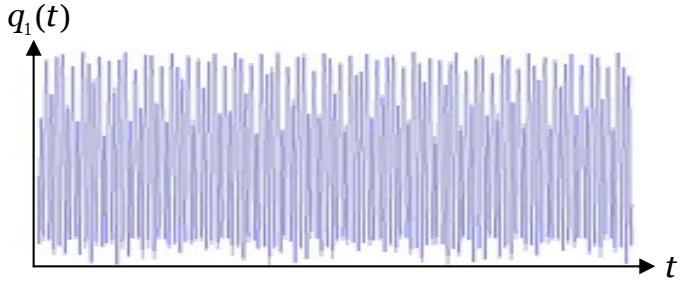


> *chaotic (?)*

> *Lyapunov exponent*

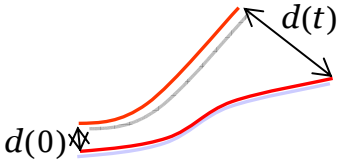


$$\lambda = \lim_{t\to\infty} \frac{1}{t} \ln \frac{d(t)}{d(0)}$$

$\lambda = 0$ regular

$\lambda > 0$ chaotic

*Questions:*

> regular or chaotic ?

> extent of chaoticity: strong or weak chaos

> intermittency: resonance trappings, transitions...

> type of chaos: slow chaos, stable chaos,...

*Who cares ?*

celestial mechanics, atomics physics
chemical physics, particle accelerators
plasma physics, ...

# *Poincaré section (2 degrees of freedom)*

individual trajectories ⟷ phase space structures

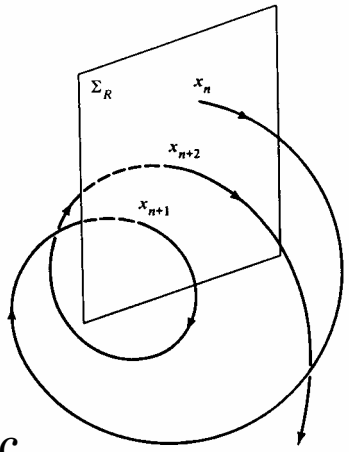


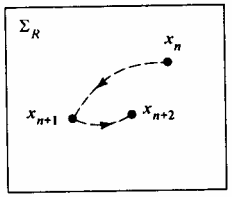


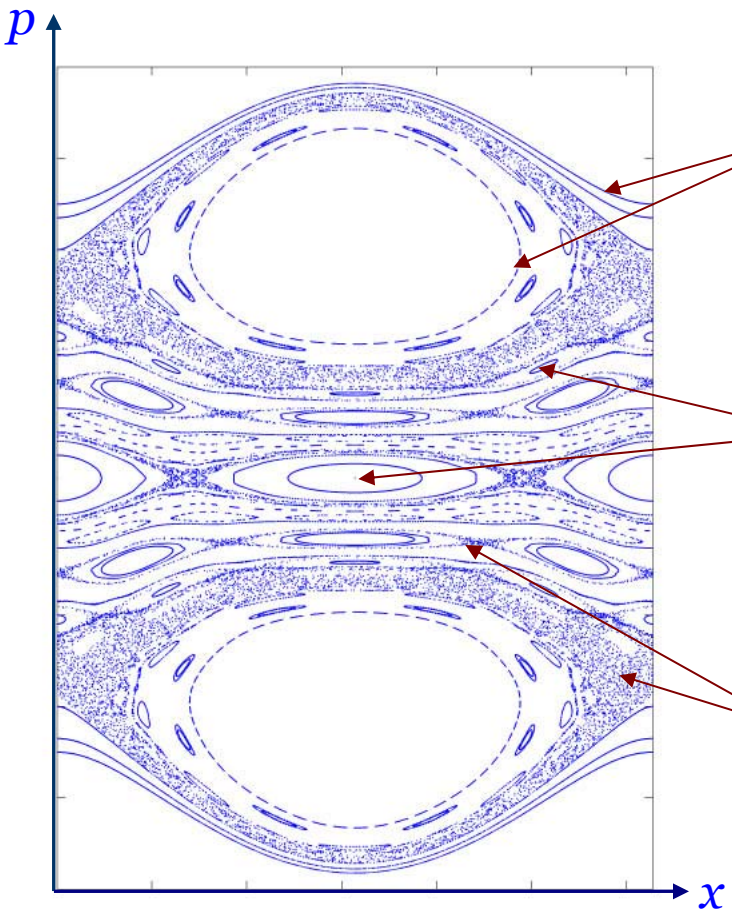


*quasiperiodic*

*periodic*

*chaotic*

> only 2 degrees of freedom
> qualitative information

$$H(p,x,t)=\frac{1}{2}p^2-\varepsilon\left(\cos x+\cos(x-t)\right)$$

# *Frequency Analysis*

> *Fourier analysis*

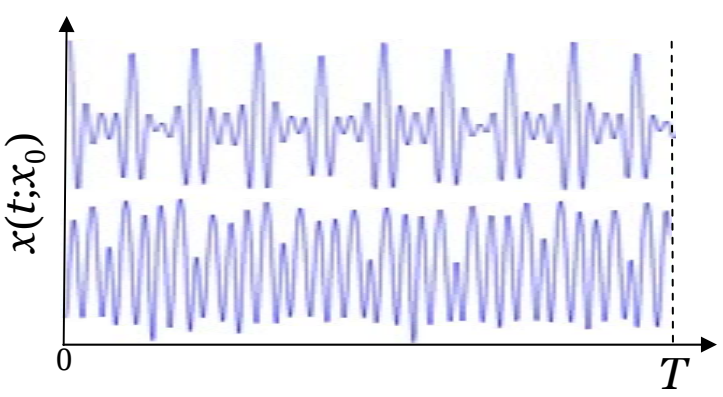


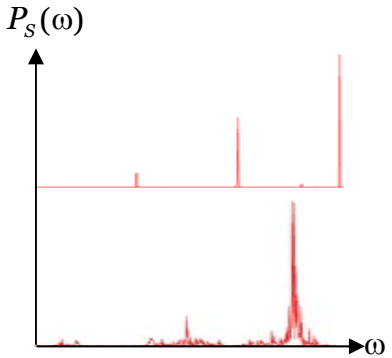


$$\Delta\omega^{FFT} = \frac{2\pi}{T}$$

> *Frequency Analysis*

Idea: decomposition of a trajectory known on a finite interval $[0,T]$ into the basis $\left\{ e^{i\omega t} \right\}_{\omega\in\mathbb{R}}$

$$\phi(\omega) = \left| \frac{1}{T}\int_0^T z(t)e^{-i\omega t}\chi(t)dt \right|^2$$

Main frequency for $z(t)$: $\omega_1$ such that $\phi(\omega_1) = \max_\omega \phi(\omega)$

without window: $\chi(t) = 1$ $\qquad \Delta\omega \propto \frac{1}{T^2}$

Hanning window: $\chi(t) = 1 - \cos\frac{2\pi t}{T}$ $\qquad \Delta\omega \propto \frac{1}{T^4}$

## *Frequency Map Analysis (J. Laskar)*

> *Fourier analysis*

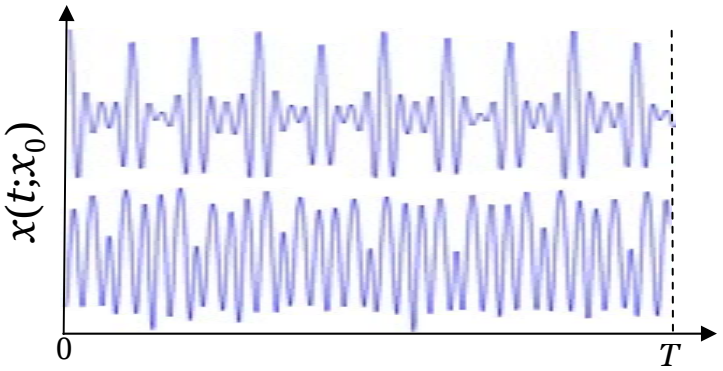


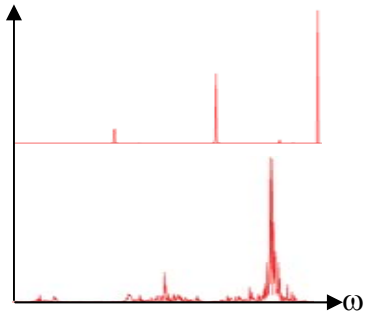


$$\delta\omega \sim \frac{1}{T}$$

> *Frequency Analysis*

Idea: decomposition of a trajectory known on a finite interval $[0,T]$ into the basis $\{e^{i\omega t}\}_{\omega\in\mathbb{R}}$

$$P_S(\omega,x_0)=\frac{1}{T}\left|\int_0^T x(t;x_0)e^{-i\omega t}\chi(t)\,\mathrm{d}t\right|$$

$$\delta\omega \sim \frac{1}{T^4}$$

periodic ✓

quasiperiodic ✓

chaotic ?

$\omega_1(x_0)$ maximizes $P_S(\bullet;x_0)$

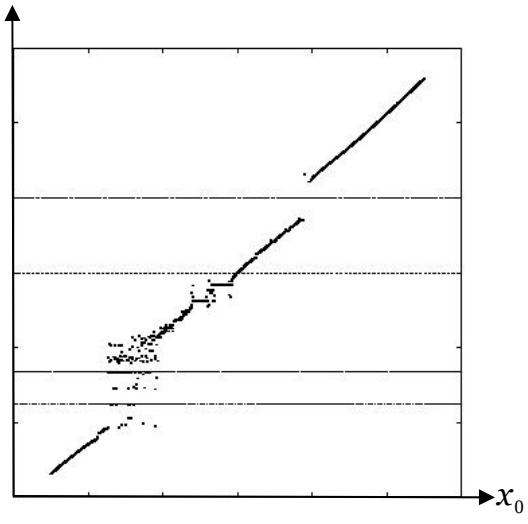


> *dynamical information, time varying frequency*

The windowed Fourier transform of *f(t)* is given by

$$Sf(u,\xi) = \int_{-\infty}^{\infty} f(t)g(t-u)e^{-i\xi t}dt$$

The Gabor transform is obtained by choosing the Gaussian window

$$g(t) = e^{-t^2/2\sigma^2} / (\sigma^2\pi)^{1/4}$$

The spectrogram is given by

$$P_S f(u,\xi) = |Sf(u,\xi)|^2$$

where

$$Sf(u,\xi) = e^{-i\xi t}\int_{-\infty}^{+\infty} f(t+u)g(t)e^{-i\xi t}dt$$

# Time-frequency resolution

The time spread around a point *(u,ξ)* in the time-frequency plane is defined as

$$\sigma_{time}(u,\xi)=\left(\int_{-\infty}^{+\infty}(t-u)^2\left|g_{u,\xi}(t)\right|^2 dt\right)^{1/2}$$

where

$$g_{u,\xi}(t)=g(t-u)e^{-i\xi t}$$

Is independent of *u* and *ξ*. For a Gaussian window $g(t)=e^{-t^2/2\sigma^2}/(\sigma^2\pi)^{1/4}$ it is equal to $\sigma/\sqrt{2}$.

The frequency spread around a point *(u,ξ)* is defined as

$$\sigma_{freq}(u,\xi)=\left(\frac{1}{2\pi}\int_{-\infty}^{+\infty}(\omega-\xi)^2\left|\hat{g}_{u,\xi}(\omega)\right|^2 d\omega\right)^{1/2}$$

Does not depend on *u* and *ξ* since $\hat{g}_{u,\xi}(\omega)=\hat{g}(\omega-\xi)e^{iu(\xi-\omega)}$.

For a Gaussian window, it is equal to $1/\sigma\sqrt{2}$.. We notice that the product of the time spread with the frequency spread at a given point *(u,ξ)* in the time-frequency plane is constant and larger than ½ (Heisenberg uncertainty). It is minimum for a Gaussian window.

## *Local Frequency Analysis*

*Observation*: chaotic motion over long time scale appears regular over shorter time scales

> intermittency

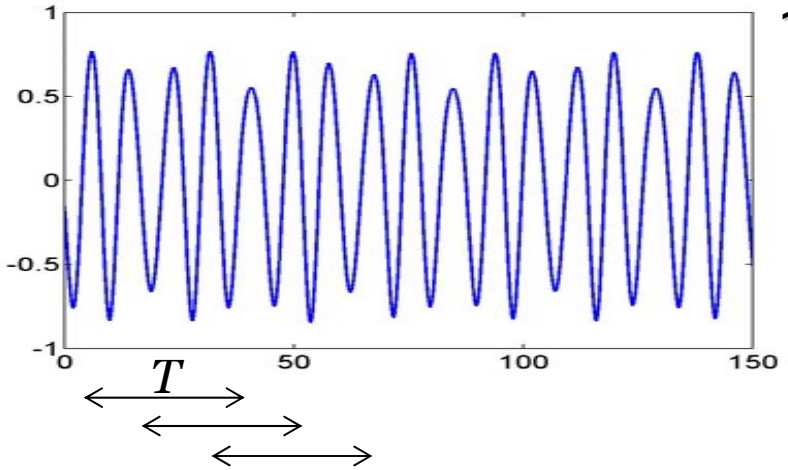


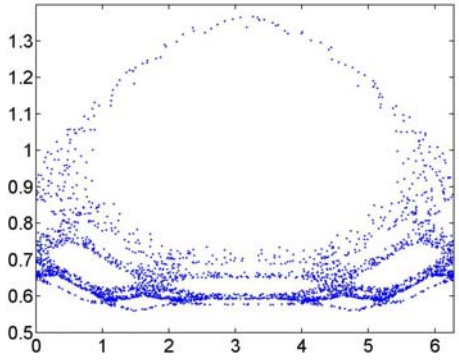

$$\phi(\omega;t) = \left| \frac{1}{T} \int_{t}^{t+T} z(t')e^{-i\omega t'} \chi(t')dt' \right| \quad \rightarrow \omega_1(t)$$

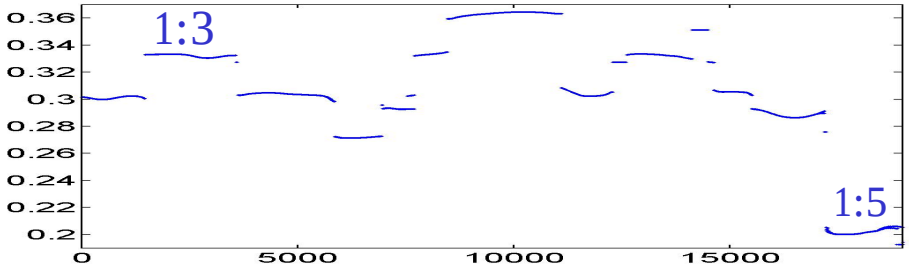


-74 dB Blackman-Harris window : $\Delta\omega \propto \frac{1}{T^2}$

Reference: Martens, Ezra, *J. Chem. Phys.* (1987)

## *Continuous Wavelet Transform*

$$Wf(u,s) = \frac{1}{\sqrt{s}} \int_{-\infty}^{+\infty} f(t) \Psi^* \left( \frac{t-u}{s} \right) dt$$

*Morlet-Grossman wavelet*

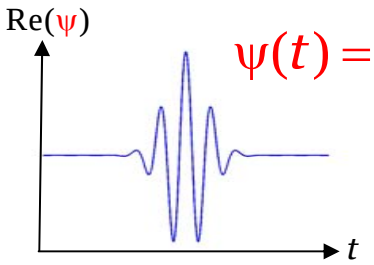


$$\psi(t) = e^{i\eta t} e^{-t^2/2\sigma^2}$$

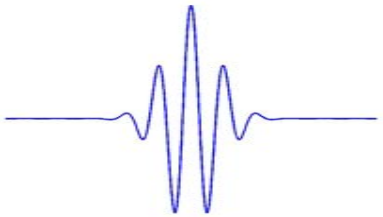

$\Psi\left(\frac{t-u}{s}\right)$ with $s > 1$

*low frequency*

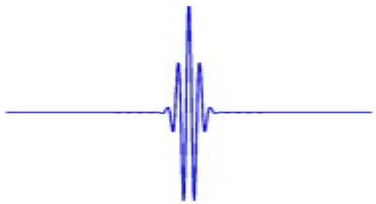

$\Psi\left(\frac{t-u}{s}\right)$ with $s < 1$

*high frequency*

Scalogram : $P_W(u,s) = \frac{1}{s} \left| Wf(u,s) \right|^2$

*Scale / frequency representation :* for $f(t) = e^{i\omega t}$, $P_W f(u,s) = e^{-\sigma^2 (s\omega - \eta)^2}$

$$\omega = \frac{\eta}{s}$$

*Fast algorithm :* $\hat{W}f(\xi,s) = \sqrt{s}\, \hat{f}(\xi) \hat{\Psi}^*(s\xi)$ $\Rightarrow$ 1 FFT + 1 IFFT

frequency resolution : $\Delta\omega \propto \frac{1}{T}$

# Continuous wavelet transform

Time-scale representation of trajectory

$$Wf(u,s) = \frac{1}{\sqrt{s}} \int_{-\infty}^{\infty} f(t) \psi^* \left( \frac{t-u}{s} \right) dt$$

Morlet-Grossman wavelet

$$\psi(t) = e^{i\eta t} e^{-t^2/2\sigma^2} / (\sigma^2 \pi)^{1/4}$$

Center frequency of wavelet

$$\eta = \frac{1}{2\pi} \int_{-\infty}^{\infty} \omega \left| \hat{\psi}_{u,s}(\omega) \right|^2 d\omega$$

$$\psi_{u,s}(t) = s^{-1/2} \psi[(t-u)/s]$$

$$\xi = \frac{\eta}{s}$$

Normalized scalogram

$$P_W f\left(u, \xi = \frac{\eta}{s}\right) = \frac{1}{s} |Wf(u,s)|^2$$

# *Time-frequency Analysis*

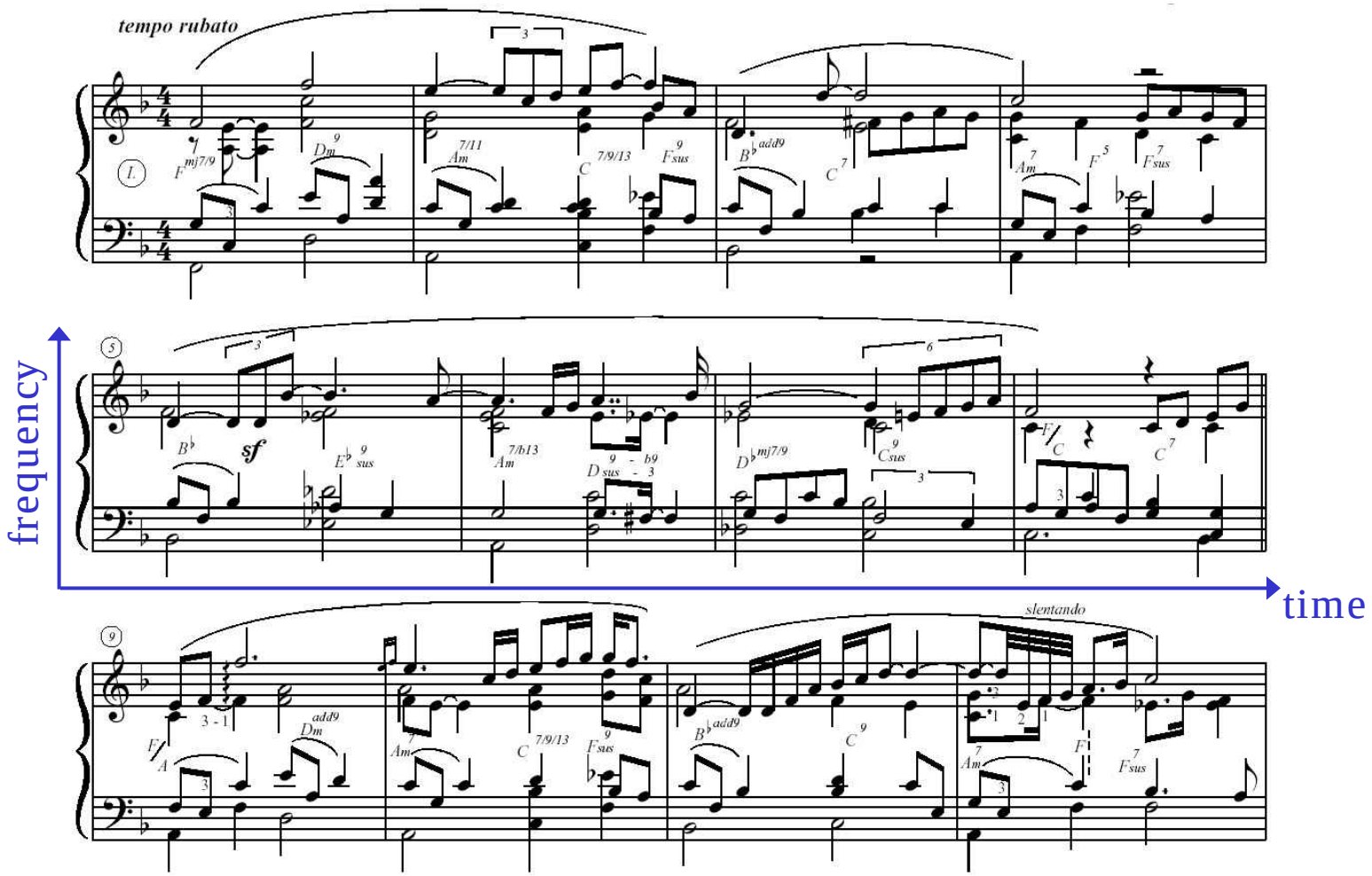


*Over the Rainbow* (Arlen/Harburg – Keith Jarrett)

For a chaotic trajectory, a ridge is a curve or a segment of curve $\xi_{loc}(u)$ in the time-frequency Which is at each time *u* a local maximum of the normalized scalogram, i.e.,

$$\left.\frac{\partial}{\partial\xi}P_W f(u,\xi)\right|_{\xi=\xi_{loc}(u)}=0, \qquad \left.\frac{\partial^2}{\partial\xi^2}P_W f(u,\xi)\right|_{\xi=\xi_{loc}(u)}<0$$

Each ridge has a weight that is the value of the normalized scalogram on this ridge (it varies continuously in time). We will refer to this value as the *amplitude* of the ridge. We call the *main ridge* or *main frequency* ridge $\xi_m(u)$ (or a set of ridges) where the normalized scalogram is a maximum:

$$P_W f(u,\xi_m(u))=\max_{\xi} P_W f(u,\xi)$$

## Instantaneous frequencies

Scalogram : $P_W(u,s) = \frac{1}{s}\left|Wf(u,s)\right|^2$

$\omega = \omega(t)$ *at time* $t = u$ $\quad \frac{\partial}{\partial\omega} P_W(u,\omega)\Big|_{\omega=\omega_{loc}(u)} = 0, \quad \frac{\partial^2}{\partial\omega^2} P_W(u,\omega)\Big|_{\omega=\omega_{loc(u)}} = 0$

*periodic trajectory*

for $f(t) = e^{i\omega t}$, $P_W f(u,s) = e^{-\sigma^2(s\omega-\eta)^2}$

$\omega = \frac{\eta}{s}$

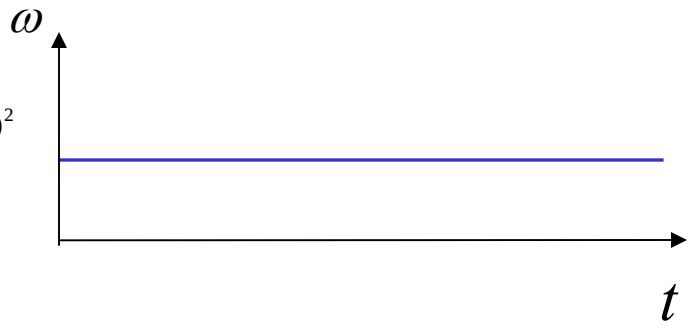


*quasiperiodic trajectory*

$f(t) = \sum_k A_k e^{i(\omega_k t + \varphi_k)}$

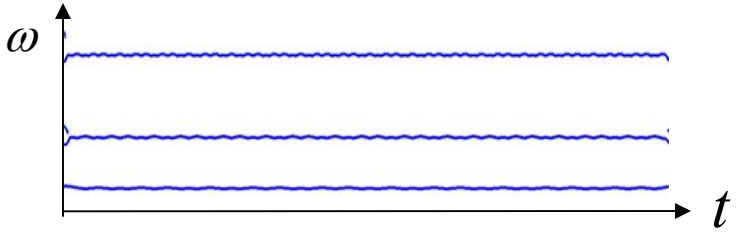


$$\tilde{\omega}_1(t) = \omega_1 + \sum_{k>1} A_k \frac{\omega_k}{\omega_1}(\omega_k - \omega_1)\cos\left[(\omega_k - \omega_1)t + \varphi_k\right] e^{-\sigma^2\eta^2(\omega_k-\omega_1)^2/2\omega_1^2}$$

Reference: C. Chandre and S. Wiggins and T. Uzer , Physica D (2003)

# *Time-frequency analysis based on wavelets*

$f(t) = \cos(\alpha t + t^2) + \cos(\beta t + \sin t)$

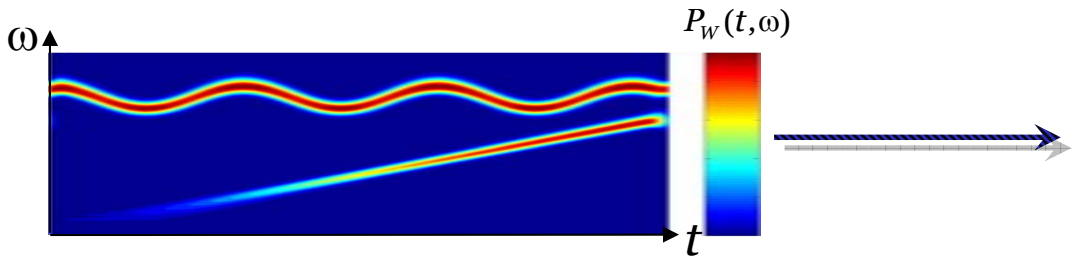


ridge extraction

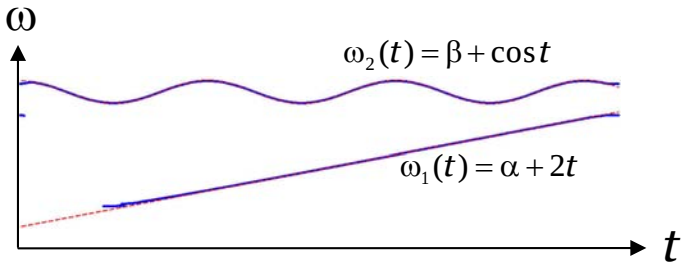


> *periodic*

$f(t) = e^{i\omega t}$

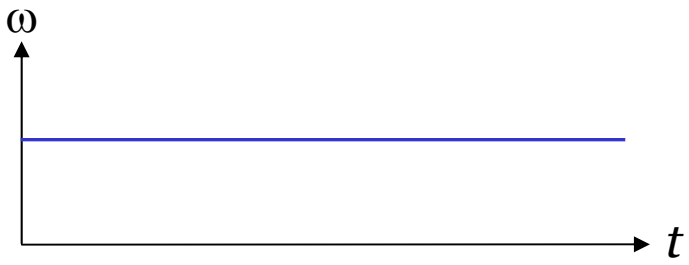


> *quasiperiodic*

$f(t) = \sum_k A_k e^{i(\omega_k t + \varphi_k)}$

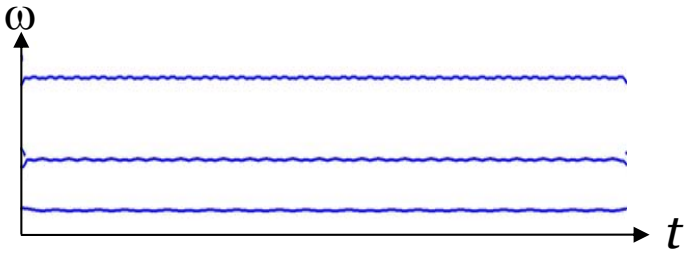


$$\tilde{\omega}_1(t) = \omega_1 + \sum_{k>1} A_k \frac{\omega_k}{\omega_1}(\omega_k - \omega_1)\cos\left[(\omega_k - \omega_1)t + \varphi_k\right] e^{-\sigma^2\eta^2(\omega_k - \omega_1)^2/2\omega_1^2}$$

Reference: Chandre, Wiggins, Uzer, *Physica D* (2003)

# Time-frequency resolution

$$\sigma_{time}(u,s) = \left( \int_{-\infty}^{+\infty} (t-u)^2 \left|\psi_{u,s}(t)\right|^2 dt \right)^{1/2}$$

Mother wavelet : $\psi(t) = e^{i\eta t} g(t)$

Gabor wavelet : $\sigma_{time} = \sigma\eta / \sqrt{2}\xi$

Frequency spread around $\xi = \eta / s$

$$\sigma_{freq}(u,s) = \left( \frac{1}{2\pi} \int_{-\infty}^{+\infty} \left( \omega - \frac{\eta}{s} \right)^2 \left|\hat{\psi}_{u,s}(\omega)\right|^2 d\omega \right)^{1/2}$$

Gabor wavelet : $\sigma_{freq} = \xi / \sigma\eta\sqrt{2}$

Heisenberg uncertainty is minimum for the Gabor wavelet

## The wavelet algorithm

$$\hat{W}f(\omega, s) = \sqrt{s}\,\hat{f}(\omega)\hat{\psi}^{*}(s\omega)$$

# Wavelet decomposition for periodic trajectory

*Poincare surface of section* ⟷ *time-frequency plane (scalogram)*

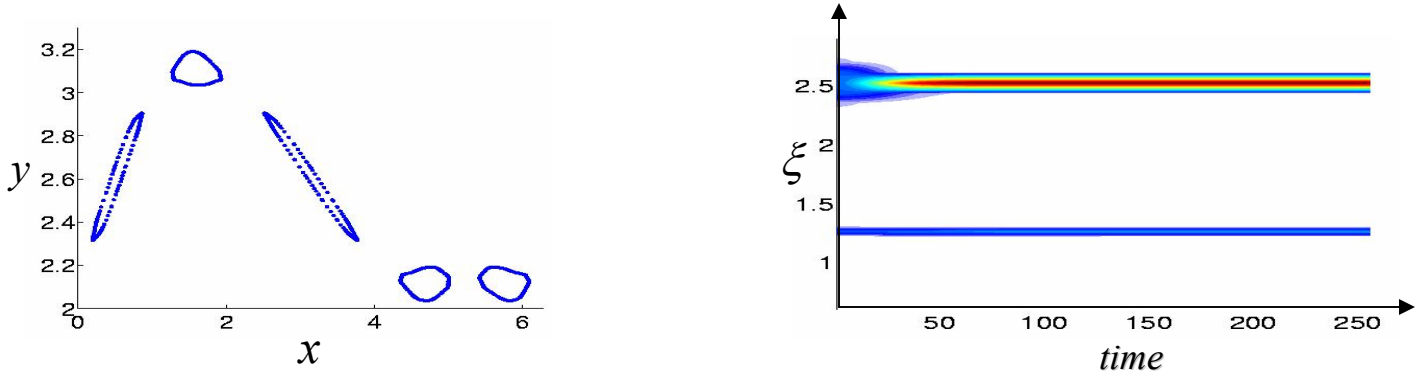


*for a periodic trajectory the maximum of scalogram is a constant curve*

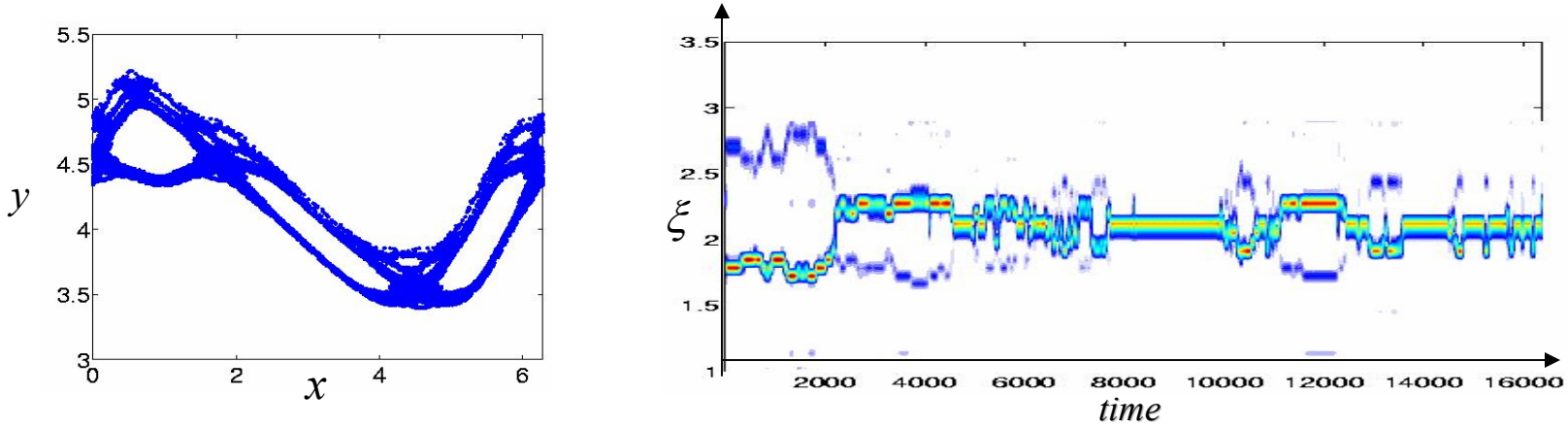


*for a chaotic trajectory the maximum of scalogram is time-dependent*

# Extraction of resonances from wavelet decomposition of a single trajectory

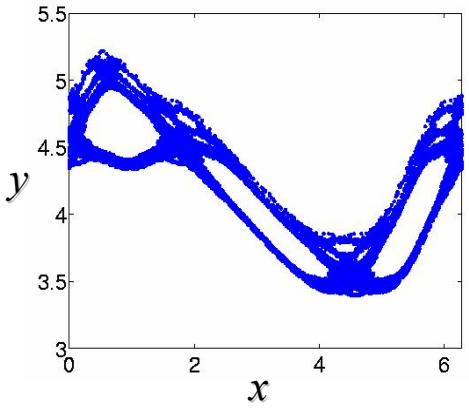


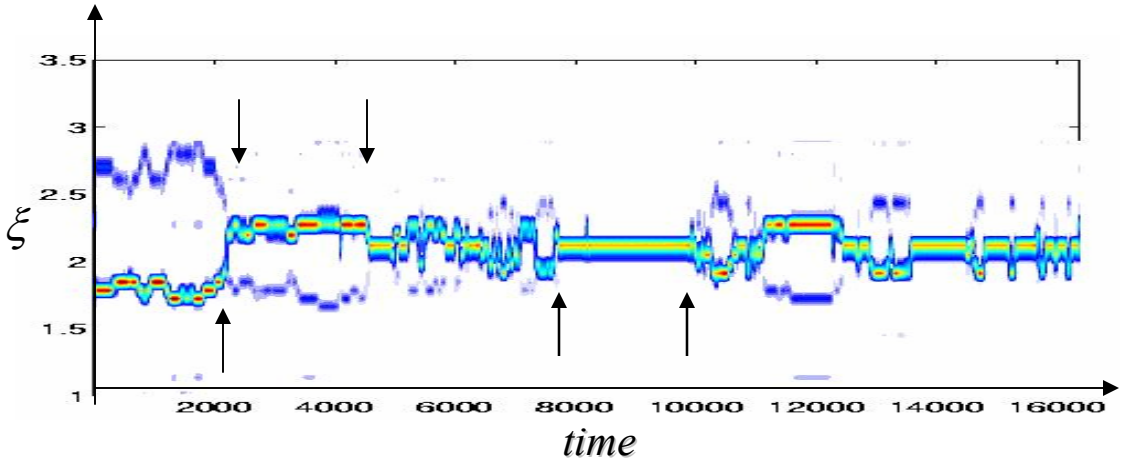


$t = [\,1,\ 2\,] \times 10^3$

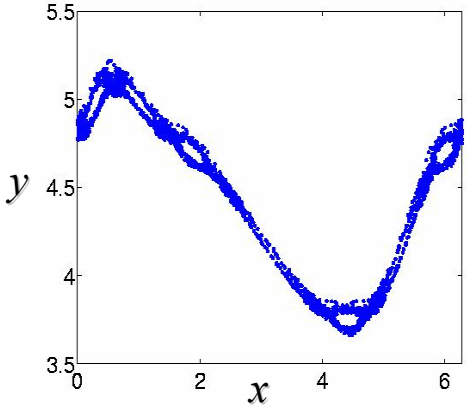


$t = [\,2,\ 4\,] \times 10^3$

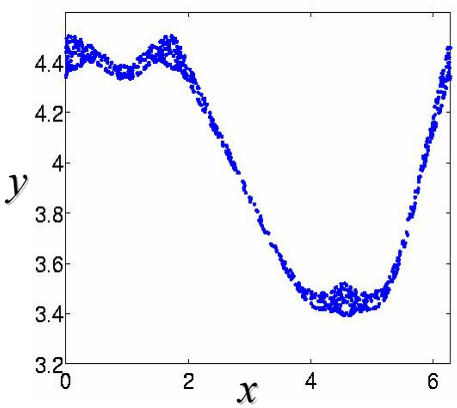


$t = [\,8,\ 10\,] \times 10^3$

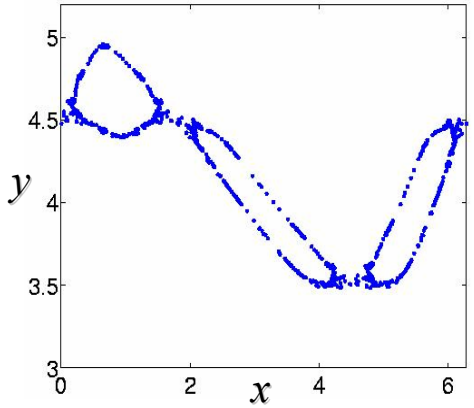

# *Rydberg atoms in crossed fields*

$$H(\boldsymbol{p},\boldsymbol{x},t)=\frac{1}{2}\|\boldsymbol{p}\|^2-\frac{1}{\|\boldsymbol{x}\|}+E(x\cos\omega t+\alpha y\sin\omega t)+\frac{B}{2}L_z+\frac{B^2}{8}\|\boldsymbol{x}\|^2$$

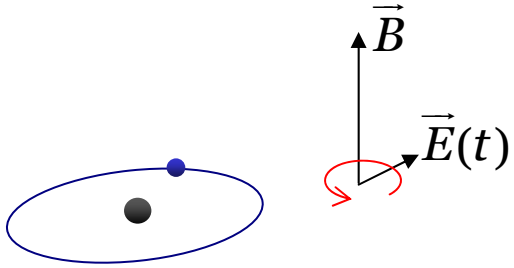


$\alpha = 0$ *linear polarization*

$\alpha = 1$ *circular polarization (2 d.o.f.)*

$\alpha \in ]0,1[$ *elliptic polarization*

**> *CPxB***

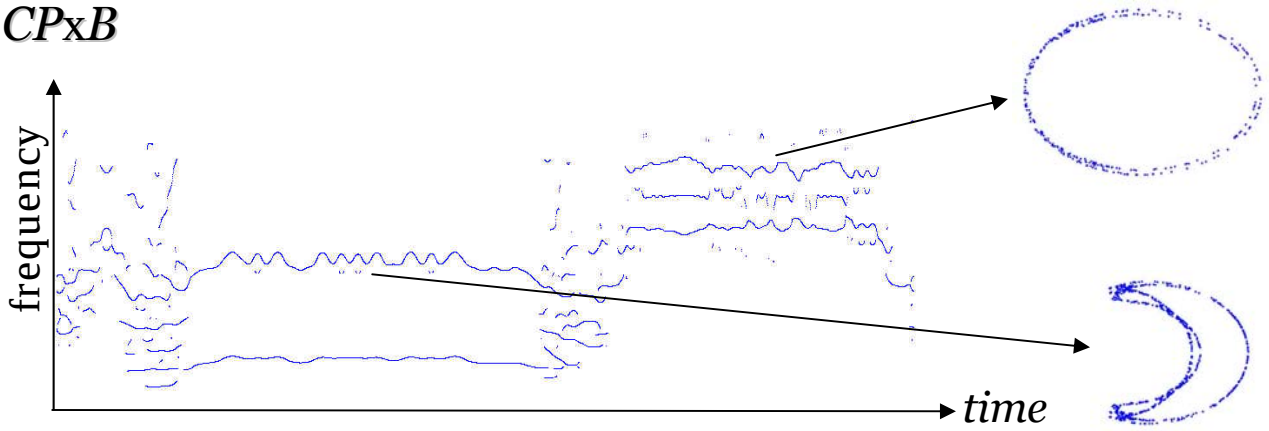


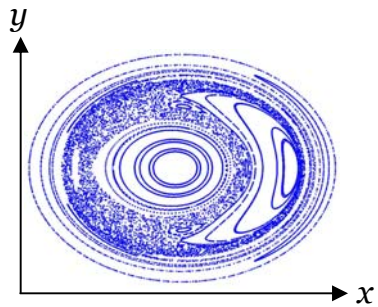


**> *EPxB***

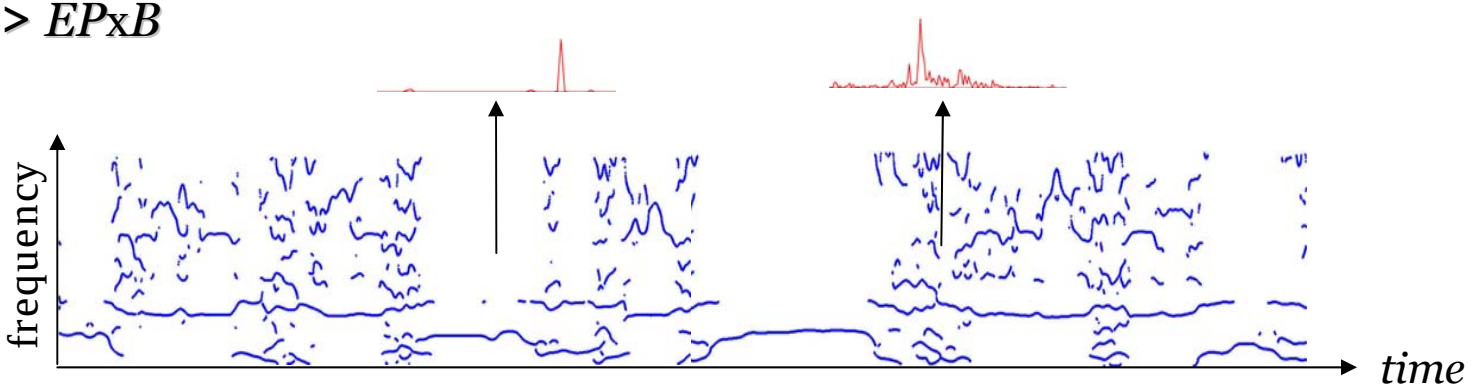

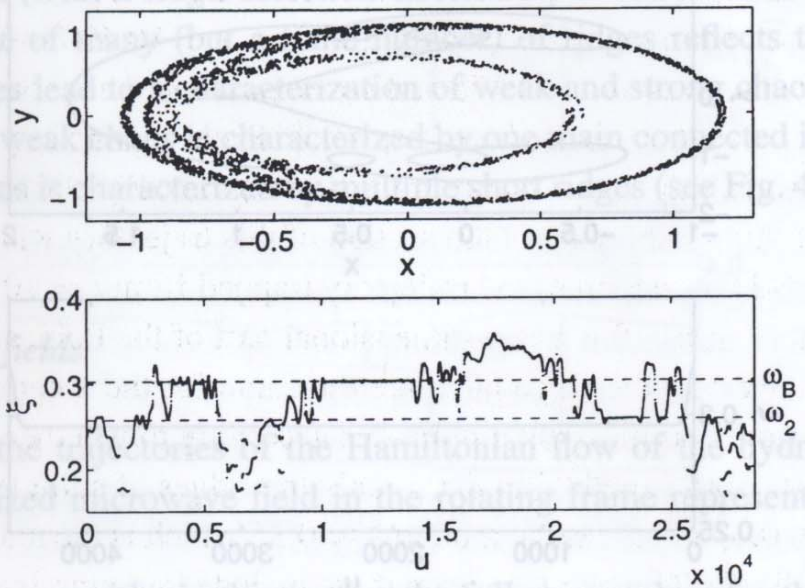


Fig. 8. Ridge plot of a chaotic orbit of Hamiltonian (9) for $F = 0.015$ and $B = 0.3$ in the maximum configuration obtained for initial conditions: $(x, y) = (-0.5, 0.7)$. The upper part of the figure represents the Poincaré section of the trajectory.

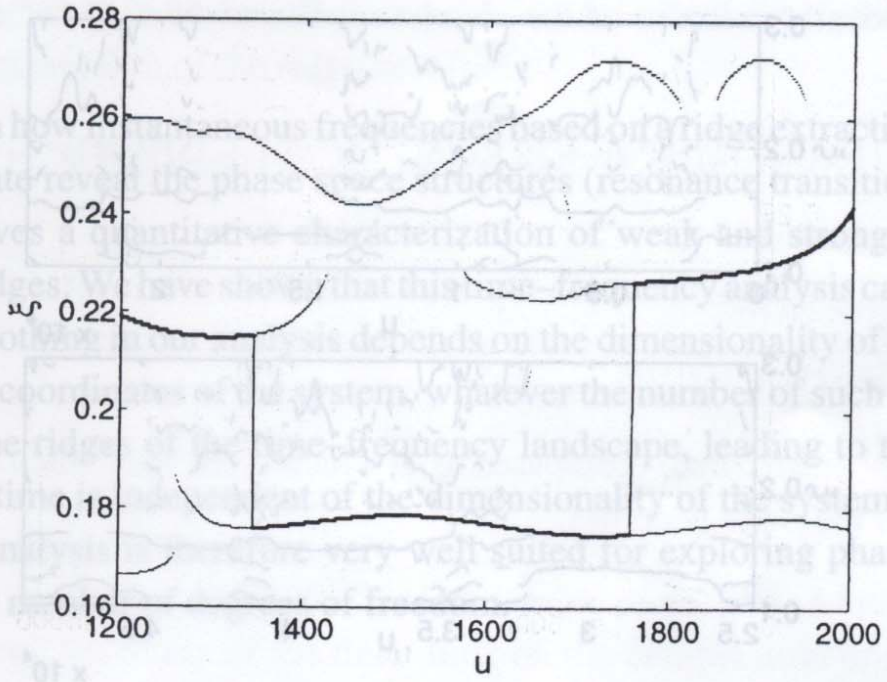


Fig. 12. Ridge plot of the same trajectory as for Fig. 8 on the time interval [1200, 2000]. The bold curve represents the main frequency curve.

# Time-frequency decomposition for strongly chaotic trajectory

*transition from resonant zone* $\omega_1 : \omega_2 : \omega_3 = 1:2:1$ *to strongly chaotic zone*

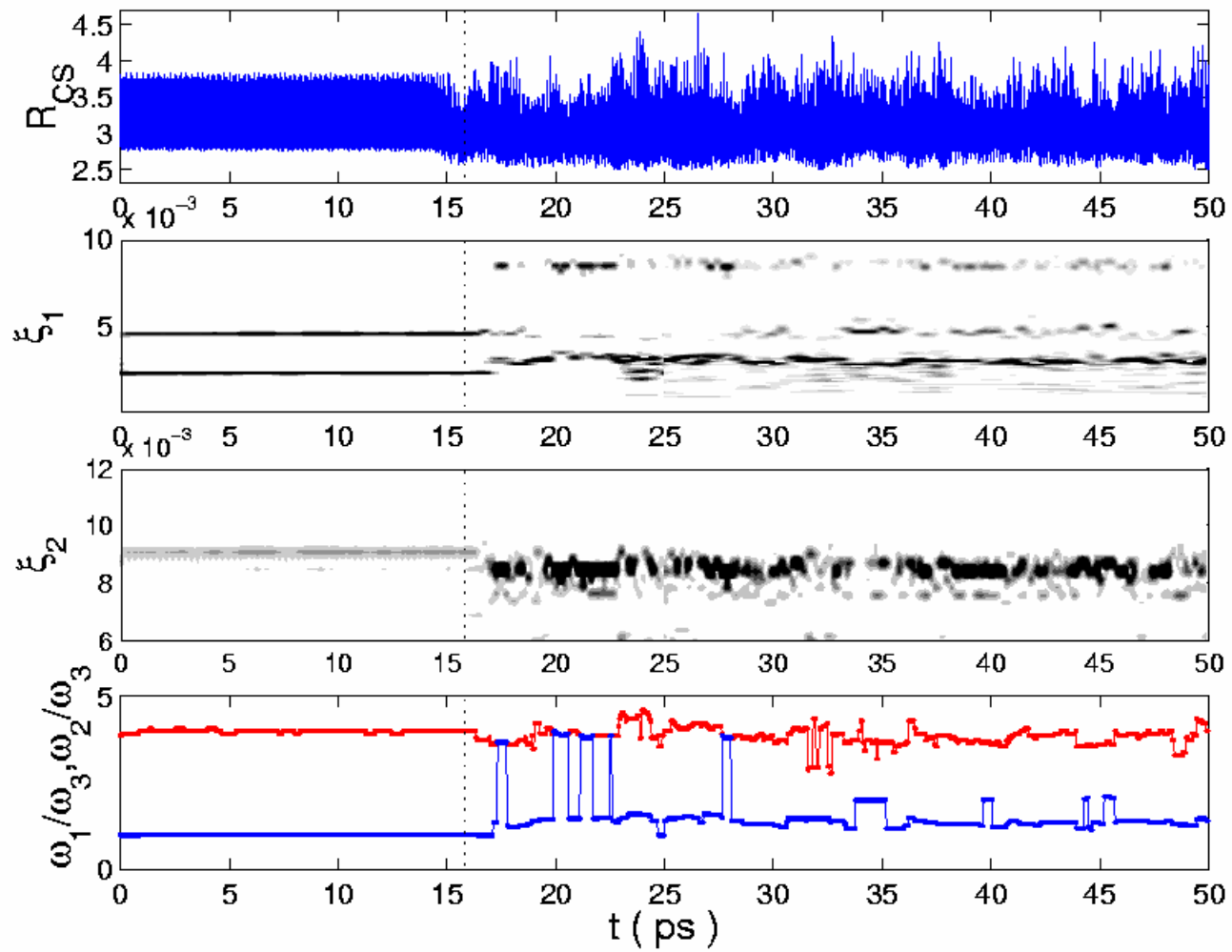

# Time-frequency decomposition for weakly chaotic trajectory

*long-time trapping for t~20 ps*

$\omega_1 : \omega_2 : \omega_3 = 2 : 4 : 1$

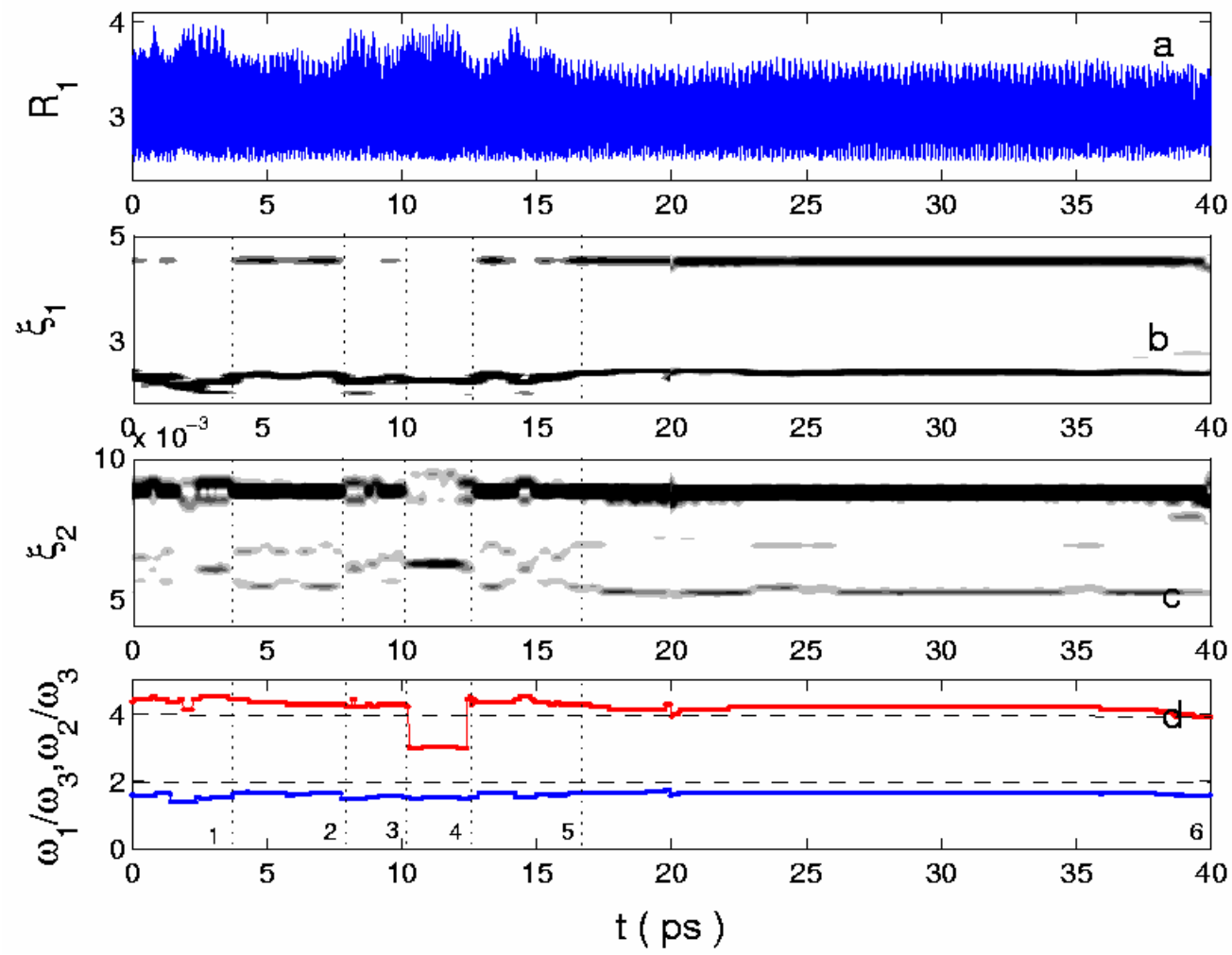

## *planar carbonyl sulfide (OCS)*

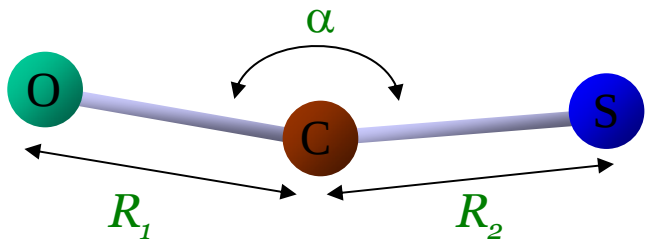


> 3 modes: OC stretch, CS stretch, OCS bend

$$H = T(P_1, P_2, P_\alpha, R_1, R_2, \alpha) + \sum_{i=1}^{3} V_m(R_i) + AP(R_1, R_2, R_3) \prod_{i=1}^{3} V_I(R_i)$$

kinetic energy — Morse — quartic polynomial — Sorbie-Murrell potential

$$T = \frac{\mu_1}{2} P_1^{\,2} + \frac{\mu_2}{2} P_2^{\,2} + \mu_3 P_1 P_2 \cos\alpha + P_\alpha^{\,2} \left( \frac{\mu_1}{2R_1^{\,2}} + \frac{\mu_2}{2R_2^{\,2}} - \frac{\mu_3 \cos\alpha}{R_1 R_2} \right) - \frac{\mu_3 P_1 P_\alpha \sin\alpha}{R_2} - \frac{\mu_3 P_2 P_\alpha \sin\alpha}{R_1}$$

$$V_m(R_i) = D_i \left( 1 - e^{-\beta_i (R_i - R_i^{\,0})} \right)^2$$

$$V_I(R_i) = 1 - \tanh\left( \gamma_i (R_i - \tilde{R}_i) \right)$$

$$P(R_1, R_2, R_3) = 1 + \sum_i c_i R_i + \sum_{i,j} c_{ij} R_i R_j + \sum_{i,j,k} c_{ijk} R_i R_j R_k + \sum_{i,j,k,l} c_{ijkl} R_i R_j R_k R_l$$

$$R_3 = \|OS\| = \sqrt{R_1^{\,2} + R_2^{\,2} - 2R_1 R_2 \cos\alpha}$$


References:

Carter, Brumer, *J. Chem. Phys.* **77** (1982), 4208
Foord, Smith, Whiffen, *Mol. Phys.* **29** (1975), 1685
Bunker, *J. Chem. Phys.* **37** (1962), 393

## *OCS potential*

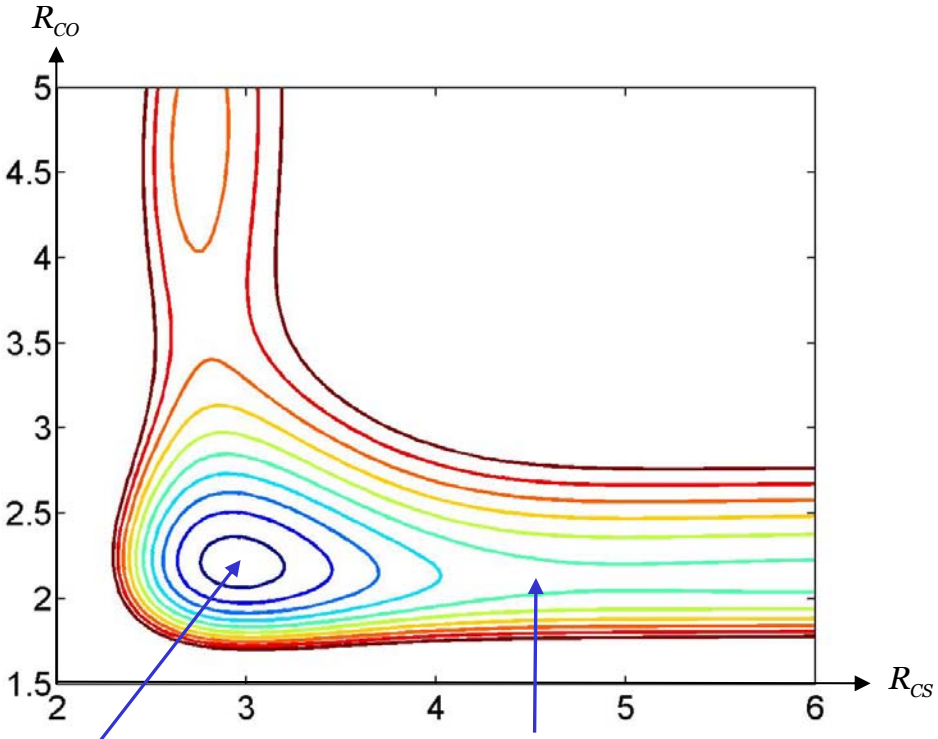


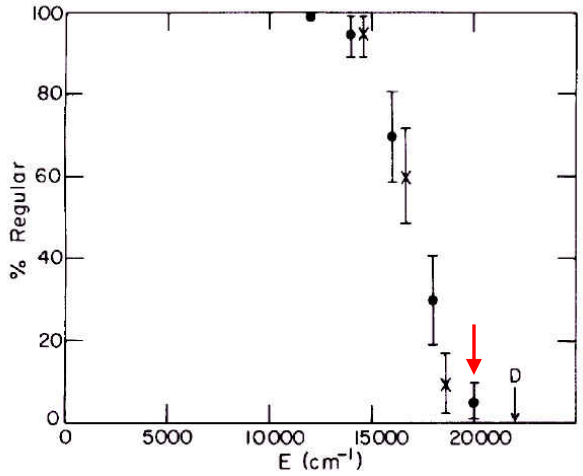


$$OCS \rightarrow OC + S \quad \text{at } E = 21900\,\text{cm}^{-1} = 0.100\,\text{a.u.}$$

equilibrium

① unimolecular dissociation of OCS

② intramolecular energy redistribution

## *Energy redistribution*

Question: time scale for energy transfer $\tau = \frac{1}{\lambda}$ ?

example: 2D coupled Morse oscillators, Henon-Heiles, cyclobutanone $C_4H_6O$

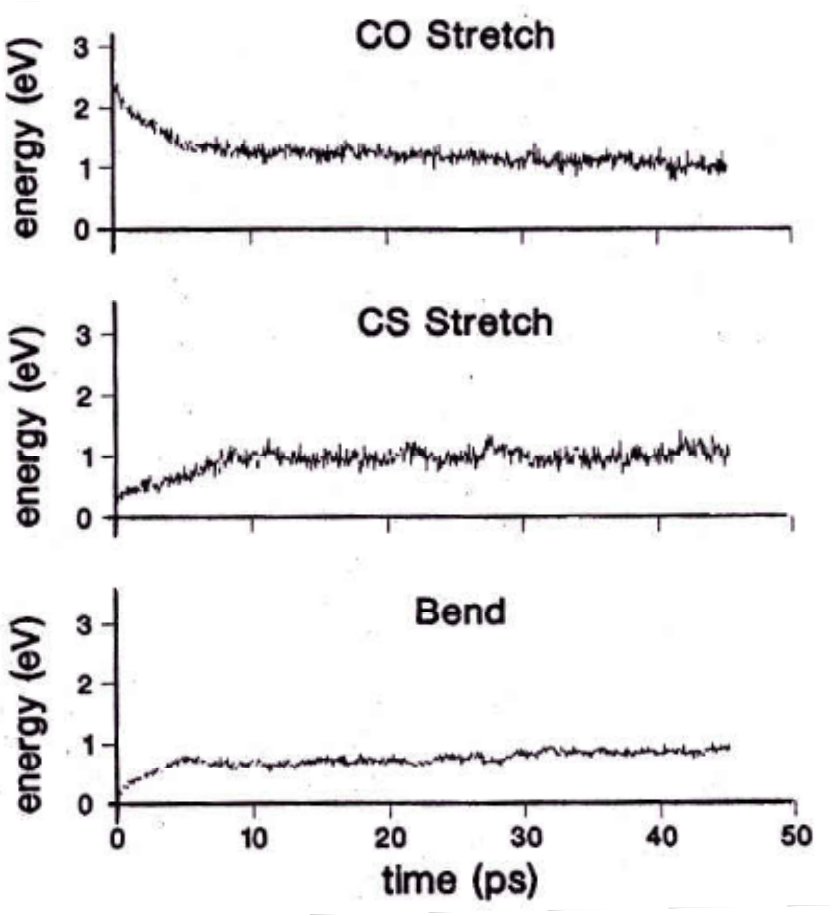


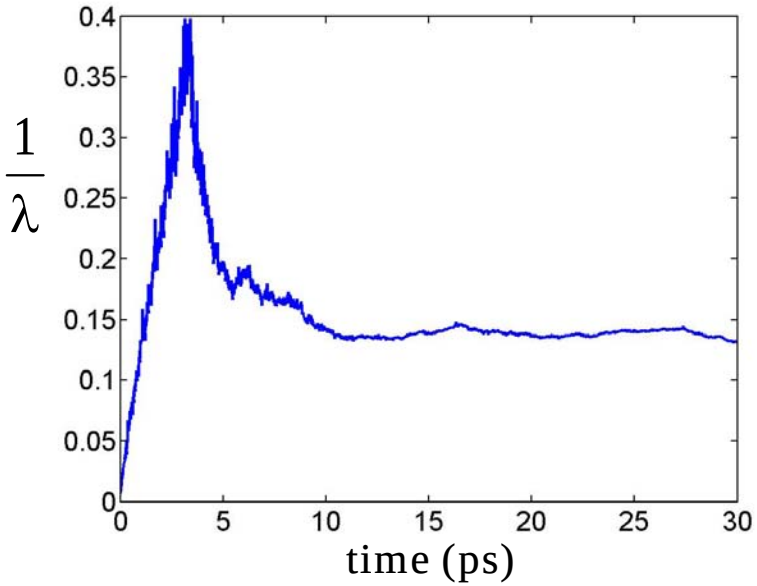


$\tau \gg \frac{1}{\lambda}$

Reference: Davis, Wagner, *ACS Symposium* (1984)

*collinear OCS (2 d.o.f.)*

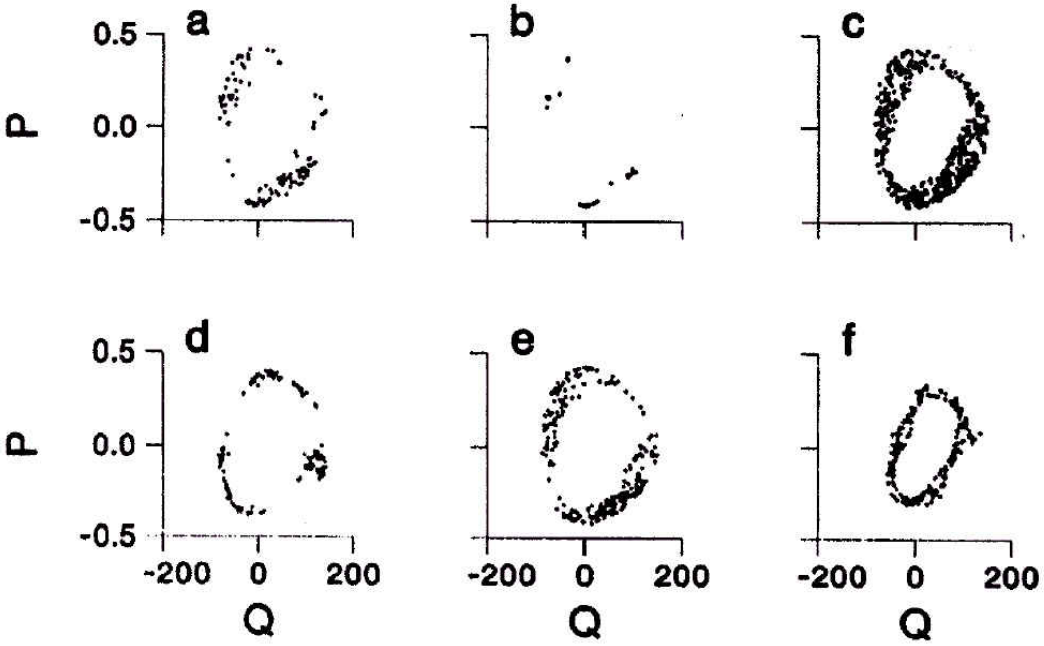


$\tau_\lambda \approx 0.1$ ps

$\tau_{ER} \approx 10$ ps

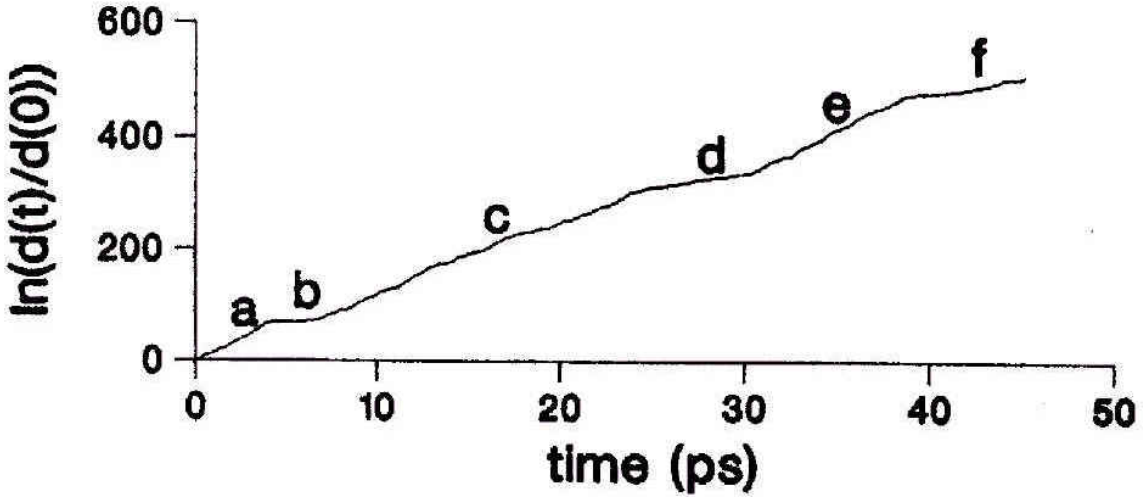


Reference: Davis, *Chem. Phys. Lett.* (1984)

*bottlenecks for collinear OCS*

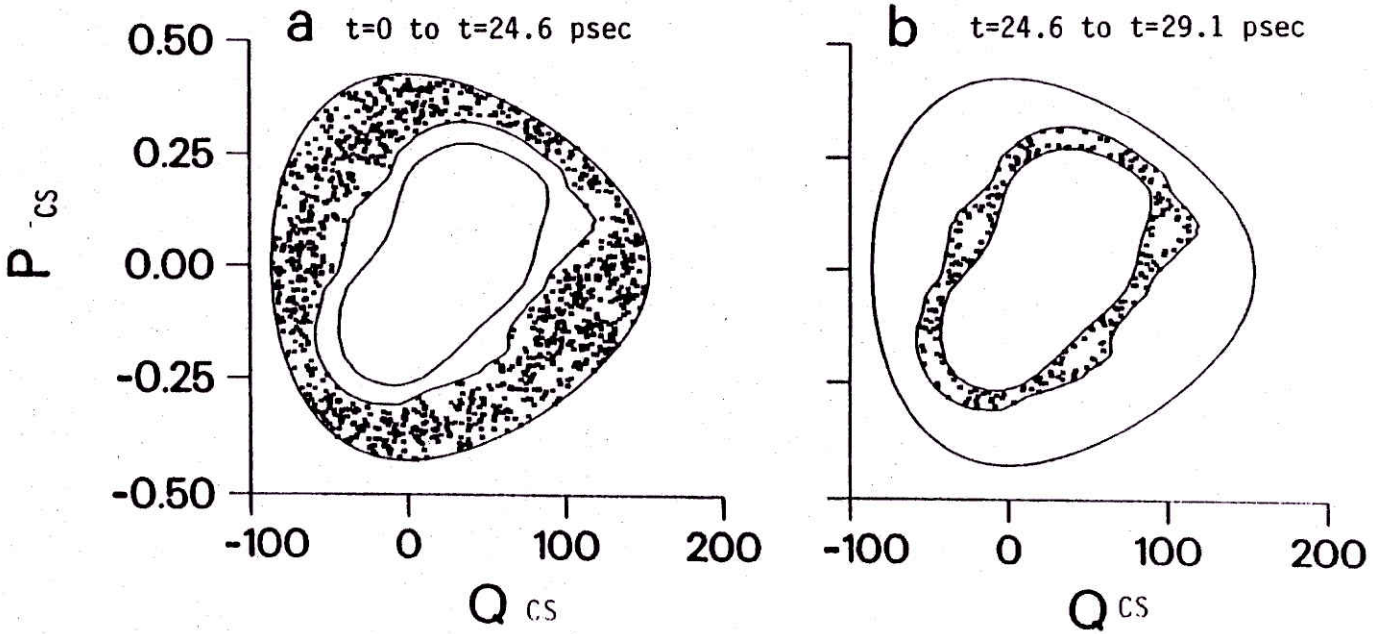


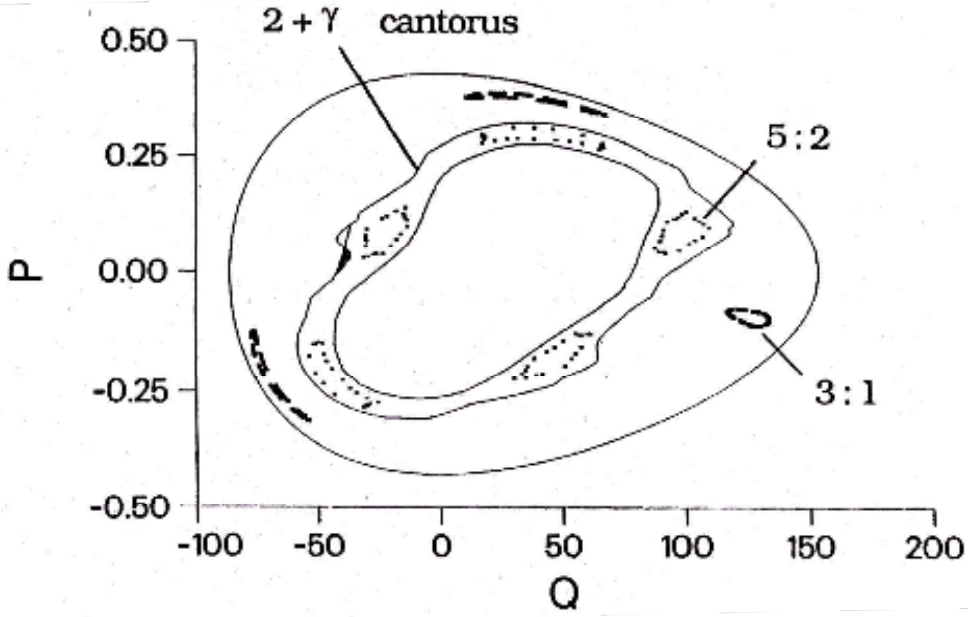

## *Frequency analysis applied to planar OCS*

> normal mode frequencies

$$\omega^0_{CO} = 2087\ \text{cm}^{-1} \quad \omega^0_{CS} = 873\ \text{cm}^{-1} \quad \omega^0_b = 520\ \text{cm}^{-1}$$

$$\xrightarrow{T = \frac{1}{c\omega}}$$

$$T^0_{CO} = 0.016\ \text{ps} \quad T^0_{CS} = 0.038\ \text{ps} \quad T^0_b = 0.064\ \text{ps}$$

$$\xrightarrow{1.4\ \text{ps}}$$

$$n_{CO} = 87 \quad n_{CS} = 36 \quad n_b = 21$$

$$\frac{\omega^0_{CO}}{\omega^0_b} \approx 4.01$$

$$\frac{\omega^0_{CS}}{\omega^0_b} \approx 1.68$$

> resonance CS/bend 3:2 *or 2:1*

> resonance CO/bend 4:1 *or 7:2*

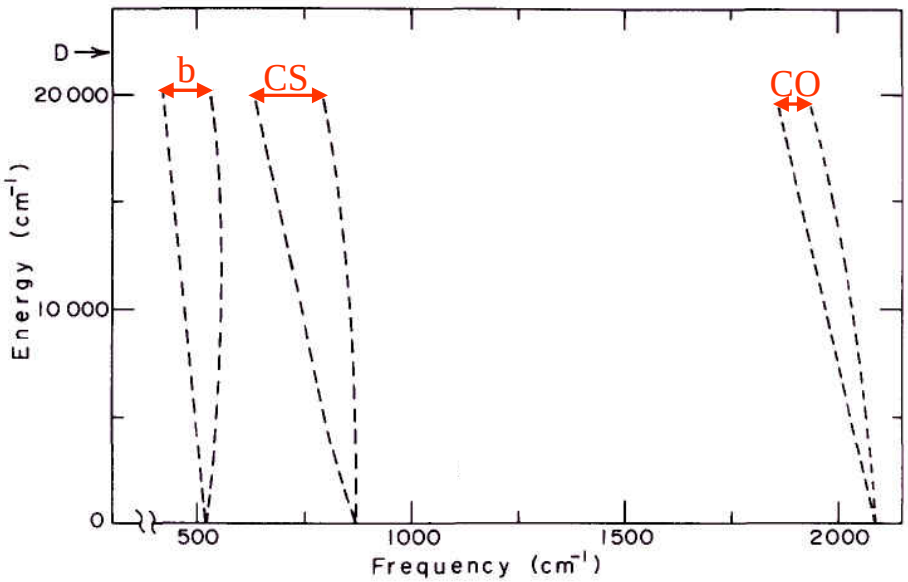


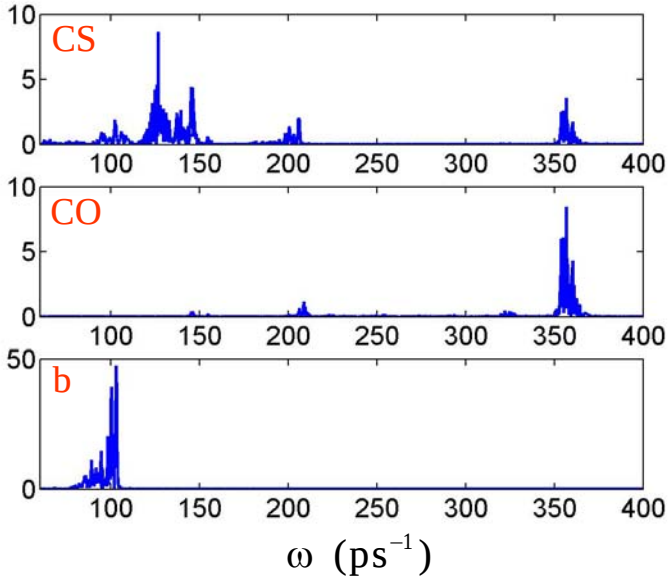

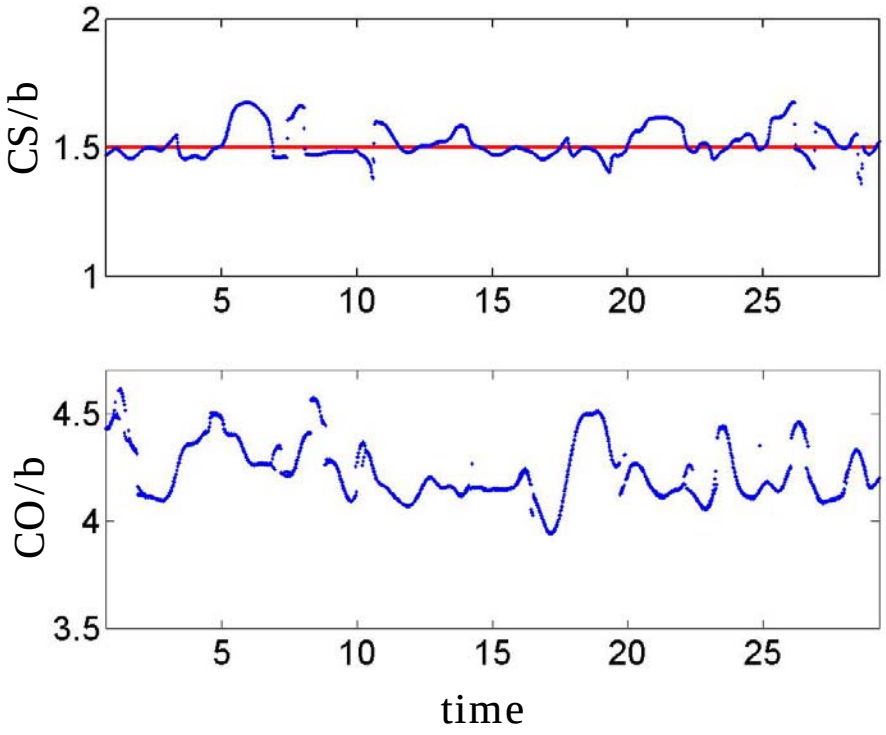


> locking of CS/bend into 3:2 resonance

> long time of resonance junctions

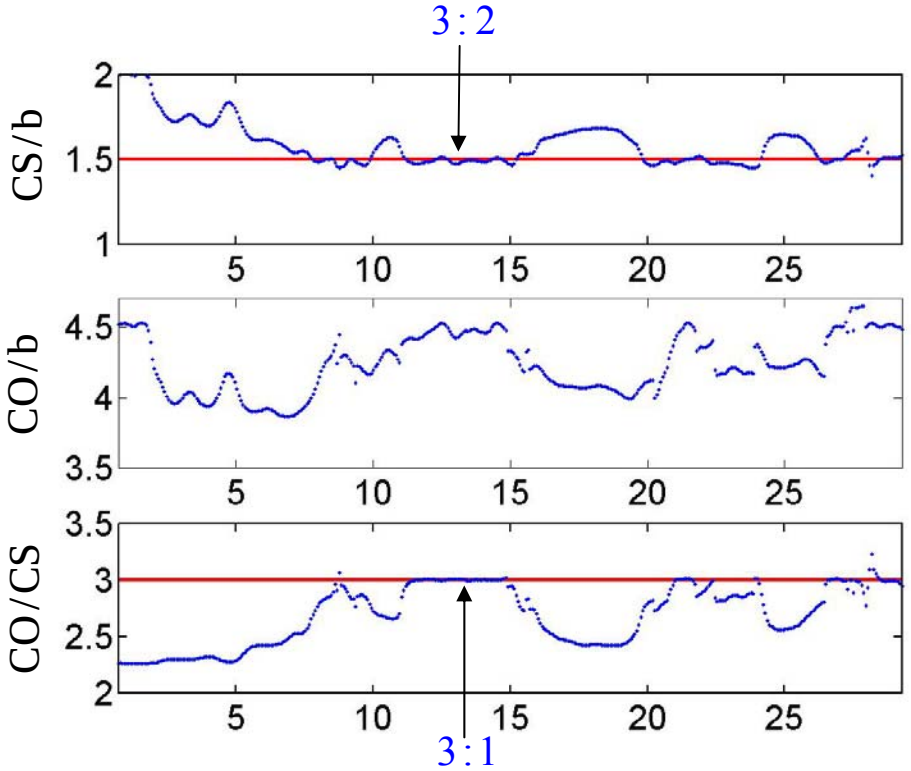

## Hamiltonian of the planar carbonyl sulfide (OCS)

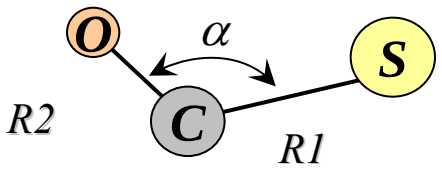


*3 modes:*
- CO stretch
- CS stretch
- $\alpha$ bend

***Hamiltonian:*** $H = T(R_1, R_2, R_3, P_1, P_2, P_3) + \sum_{i=1}^{3} V_i(R_i) + V_{INT}(R_1, R_2, R_3),$

*kinetic term* — *Morse potential* — *Sorbie-Murrell term*

$$T = \frac{1}{2\mu_1} P_1^2 + \frac{1}{2\mu_2} P_2^2 + \frac{1}{\mu_3} P_1 P_2 \cos\alpha + P_\alpha^2 \left( \frac{1}{2\mu_1 R_1^2} + \frac{1}{2\mu_2 R_2^2} - \frac{\cos\alpha}{\mu_3 R_1 R_2} \right) - \frac{P_1 P_\alpha \sin\alpha}{\mu_3 R_2} - \frac{P_2 P_\alpha \sin\alpha}{\mu_3 R_1},$$ where $\mu_i$ are the reduced masses

### *Sorbie-Murrell interaction term:*

$$V_{INT}(R) = A\, P(\Delta R_1, \Delta R_2, \Delta R_3) \prod_{i=1}^{3} \left[ 1 - \tanh\left( \frac{\gamma_i \Delta R_i}{2} \right) \right]$$

$\Delta R_i = R_i - \tilde{R}_i$, $R_3 = \sqrt{R_1^2 + R_2^2 - 2R_1 R_2 \cos(\alpha)}$, $P(\Delta R_1, \Delta R_2, \Delta R_3)$ is a quartic polynomial

$$P(s_1, s_2, s_3) = 1 + \sum_i c_i s_i + \sum_{i,j} c_{ij} s_i s_j + \sum_{i,j,k} c_{ijk} s_i s_j s_k + \sum_{i,j,k,l} c_{ijkl} s_i s_j s_k s_l,$$

where $s_i = R_i - \tilde{R}_i$, $\tilde{R}_i$ are the equilibrium distances for the collinear case

# OCS potential surface

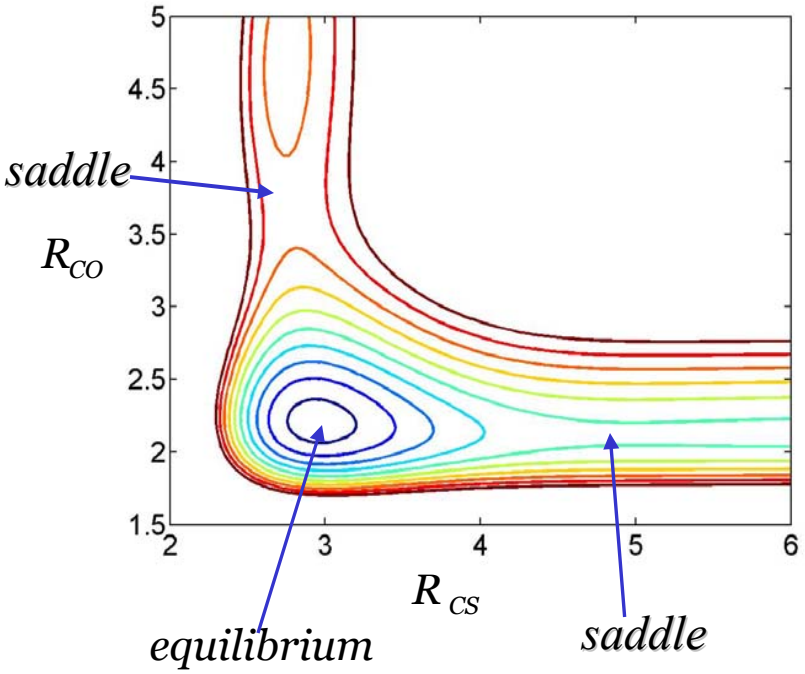


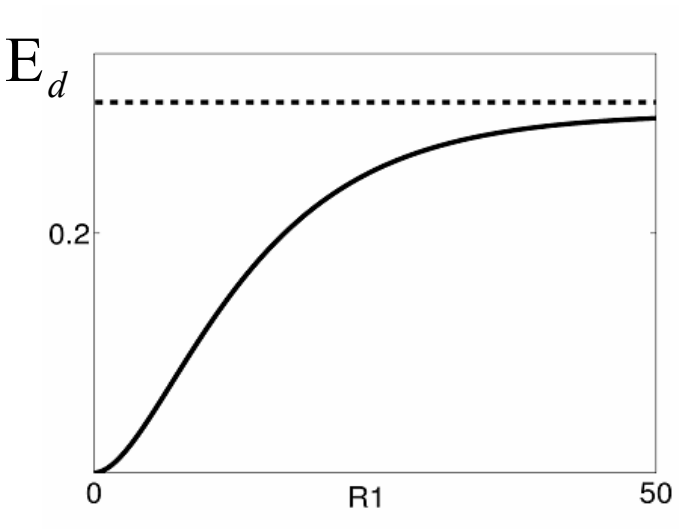


$$R_3 = \sqrt{R_1^2 + R_2^2 - 2R_1R_2\cos(\alpha)}$$

$$E_d = V(R_1 \to \infty, R_2, R_3) = \sum_{i=1}^{3} D_i \left(1 - e^{-\beta_i (R_i - R_i^0)}\right)^2 = D_1 + D_3 + D_2 (1 - e^{-\beta_2 (R_2 - R_2^0)})^2$$

$$E_d \geq D_1 + D_3 = 0.1 \text{ a.u.}$$

$$OCS \to OC + S \quad \text{at } E = 21\,900 \text{ cm}^{-1} = 0.100 \text{ a.u.}$$

## Phase space bottlenecks to long-time energy relaxation

*intramolecular energy relaxation are related to phase space structures*

M. J. Davis, *J. Chem. Phys.*, **83,** 1016, (1985)

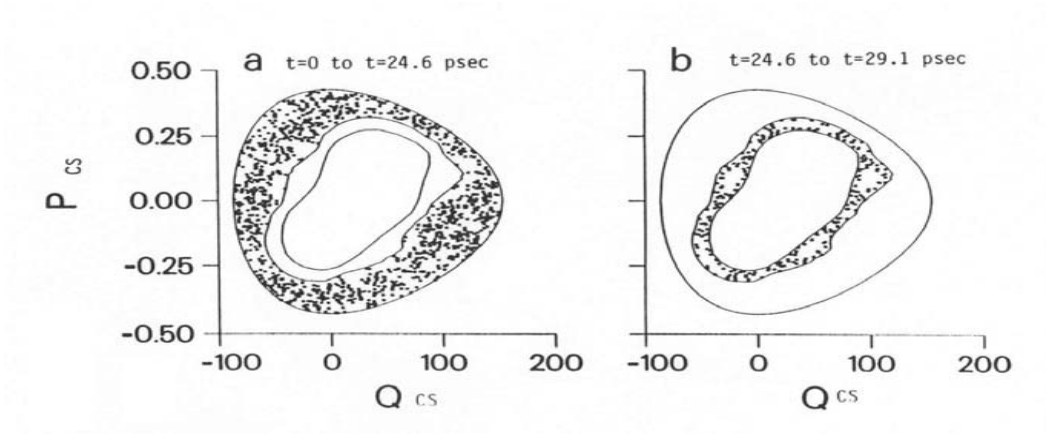


$\gamma = (\sqrt{5} + 3)/2,$

$2.5 \le \gamma \le 3$

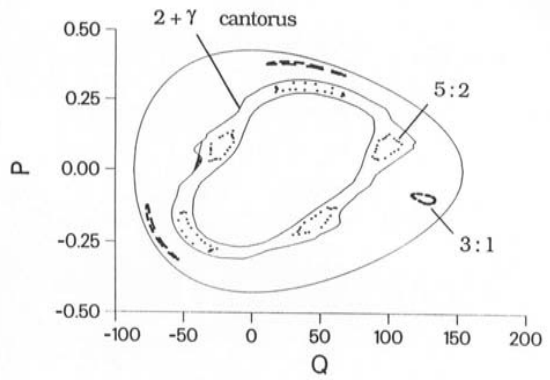


## ***Barriers for diffusion of trajectories***

*2-DOF system*

*3D constant energy surface*

*2D invariant tori*

*3-DOF system*

*5D constant energy surface*

*3D invariant tori*

*barrier to chaotic transport in 3-DOF system is 4D subspace:* $F(\omega) = 0$

*Reference:* C. C. Martens, *et al, Chem. Phys. Lett.*,**142,** 519, (1987)

# Periodic orbits and invariant tori

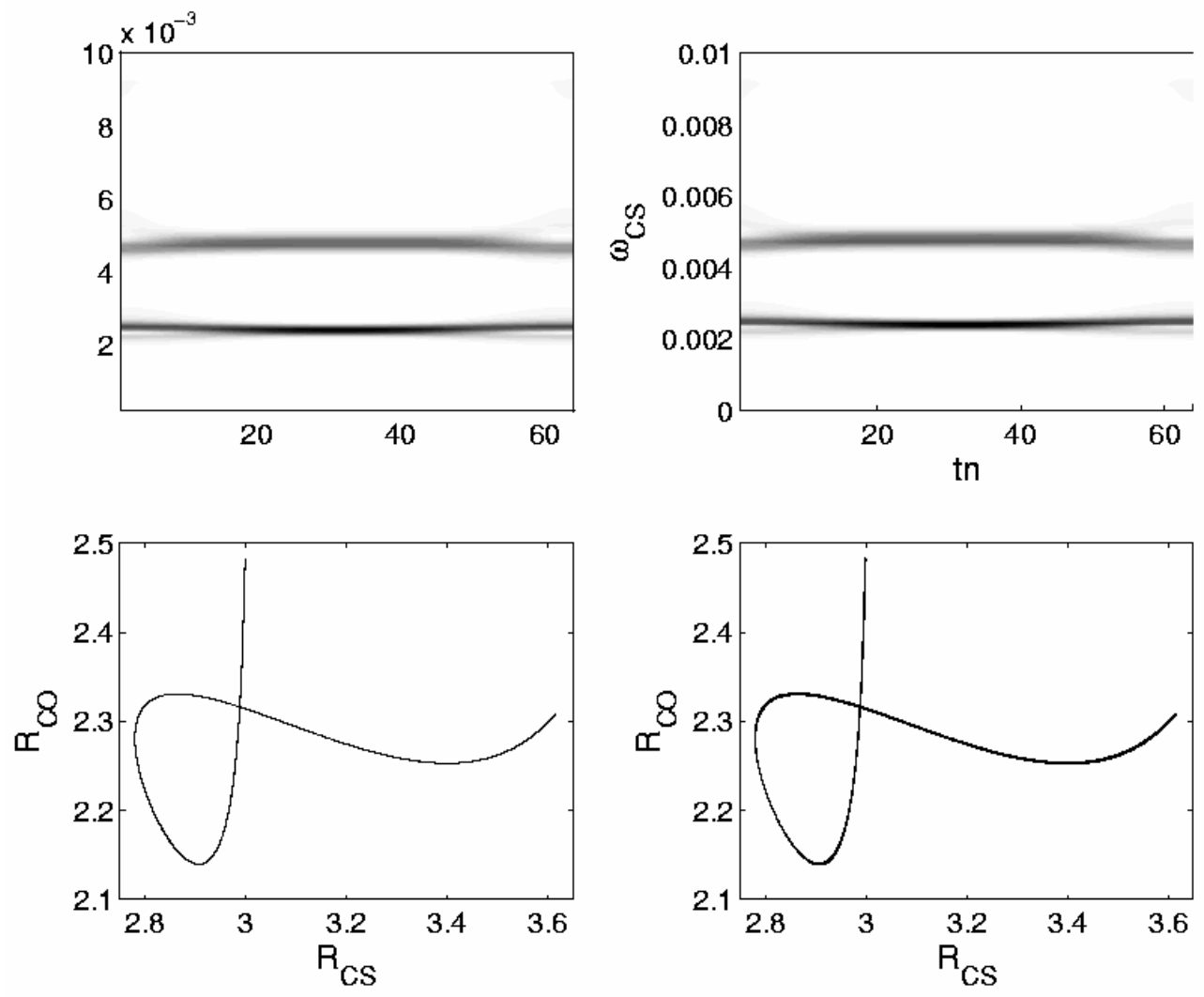

# Time-frequency analysis for hydrogen in EP fields

## *Periodic trajectory*

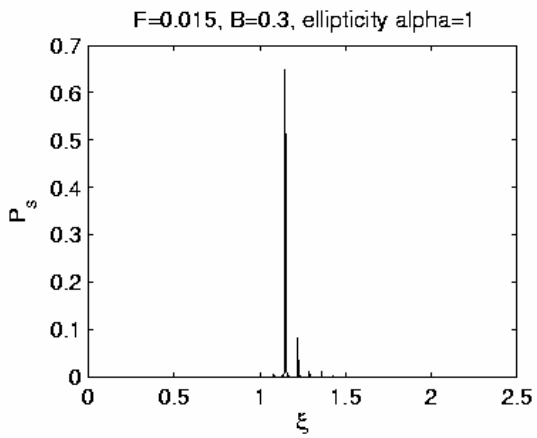


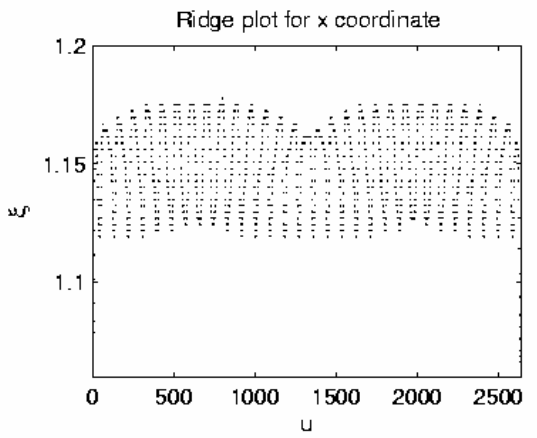


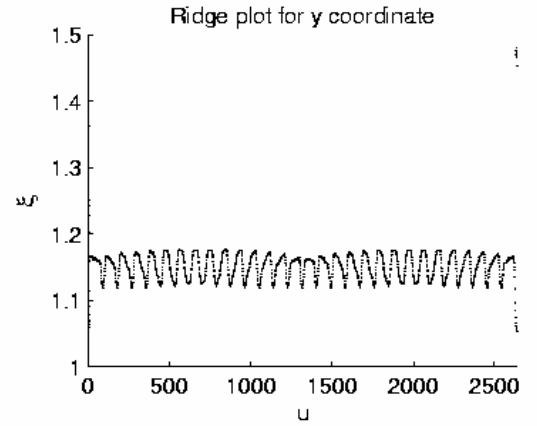


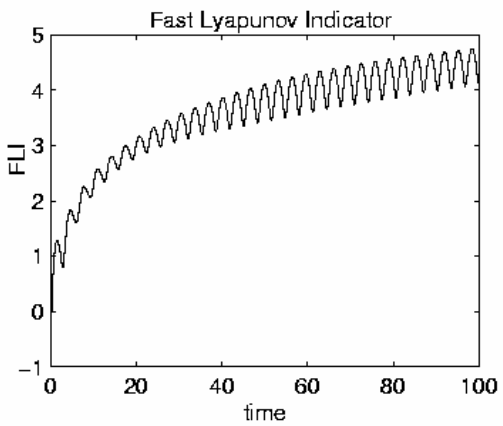

# Spectral data versus FLI results

*weakly chaotic trajectory*

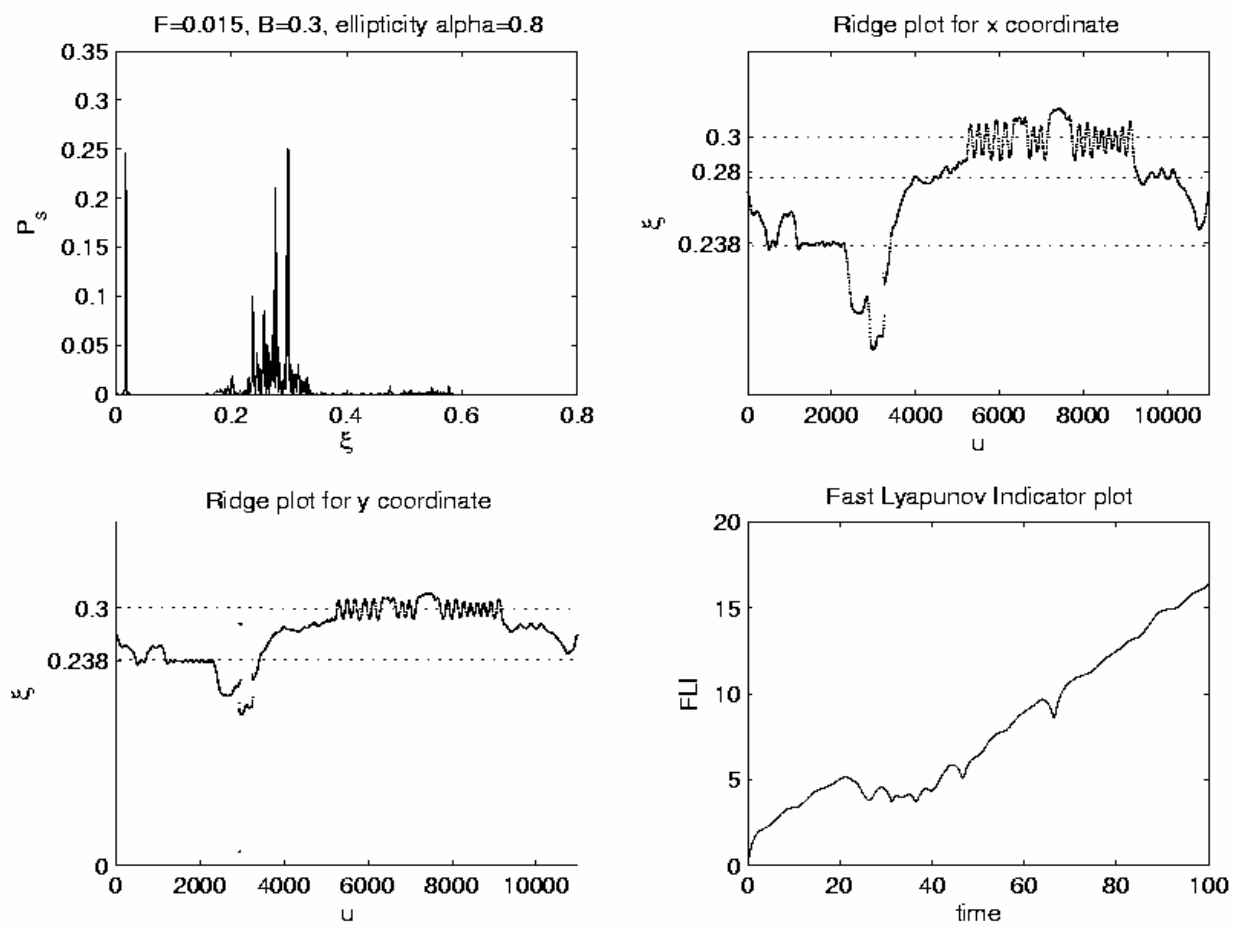

# Spectral data versus FLI results

*strongly chaotic trajectory*

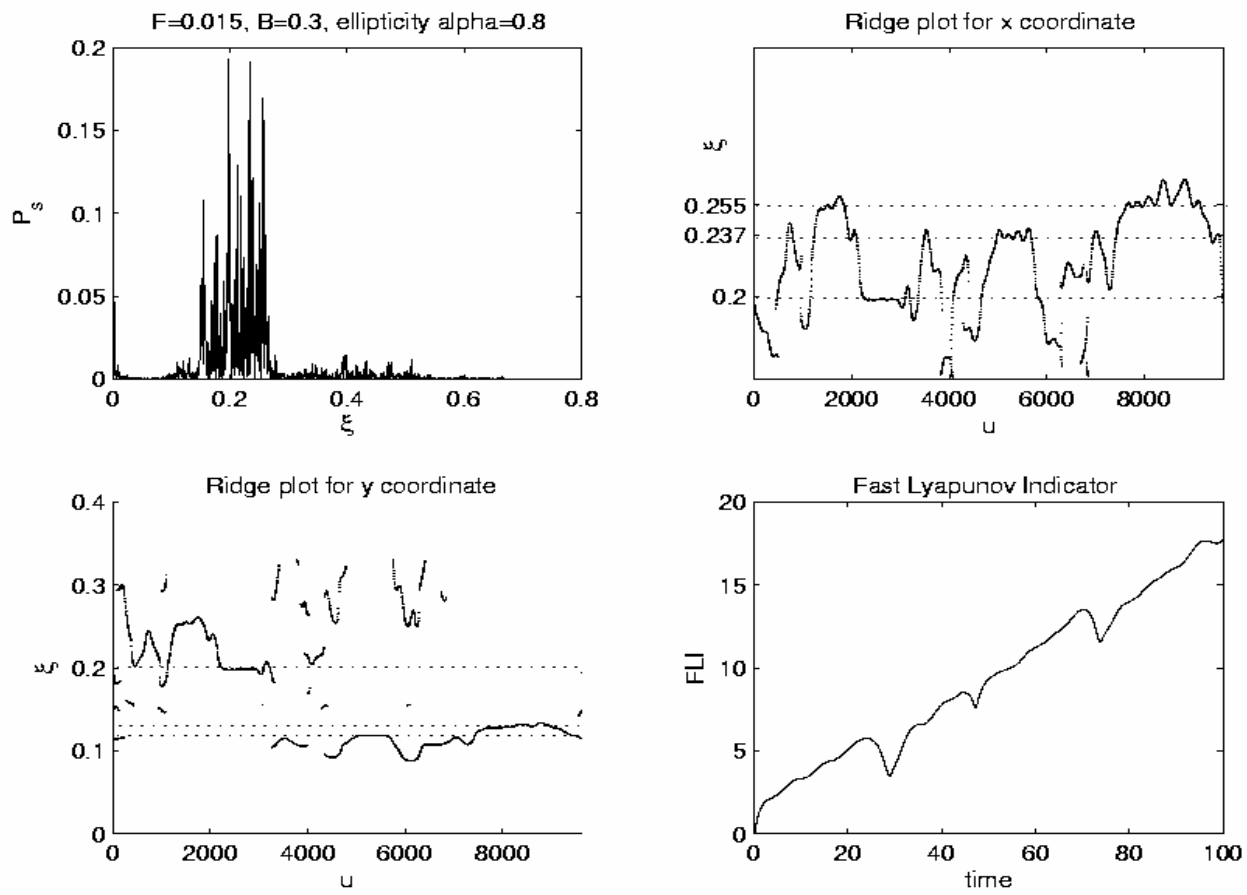

# Time-frequency planes for 3D hydrogen in crossed fields

*weakly chaotic trajectory*

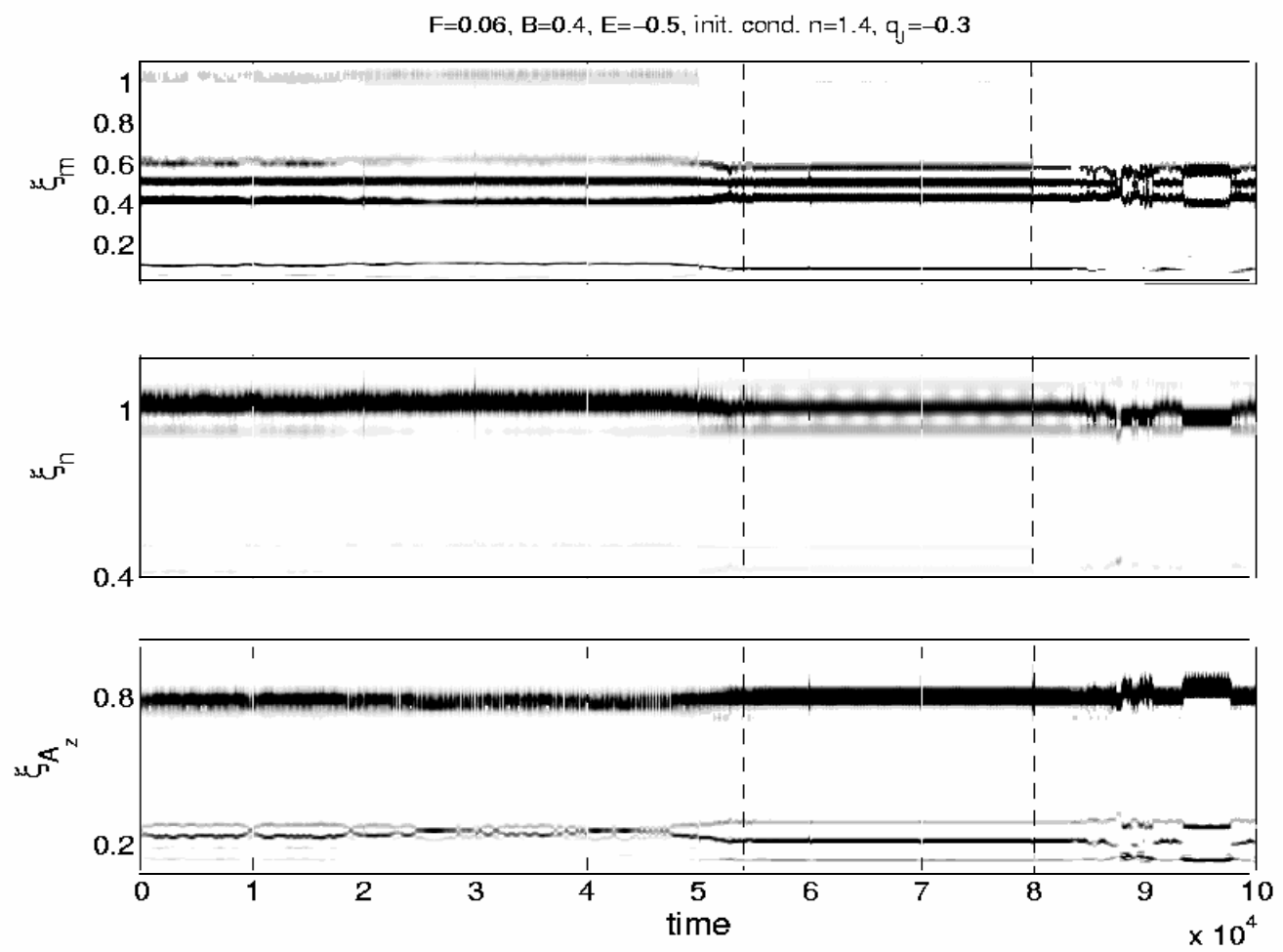

# Time-frequency planes for strongly chaotic trajectory

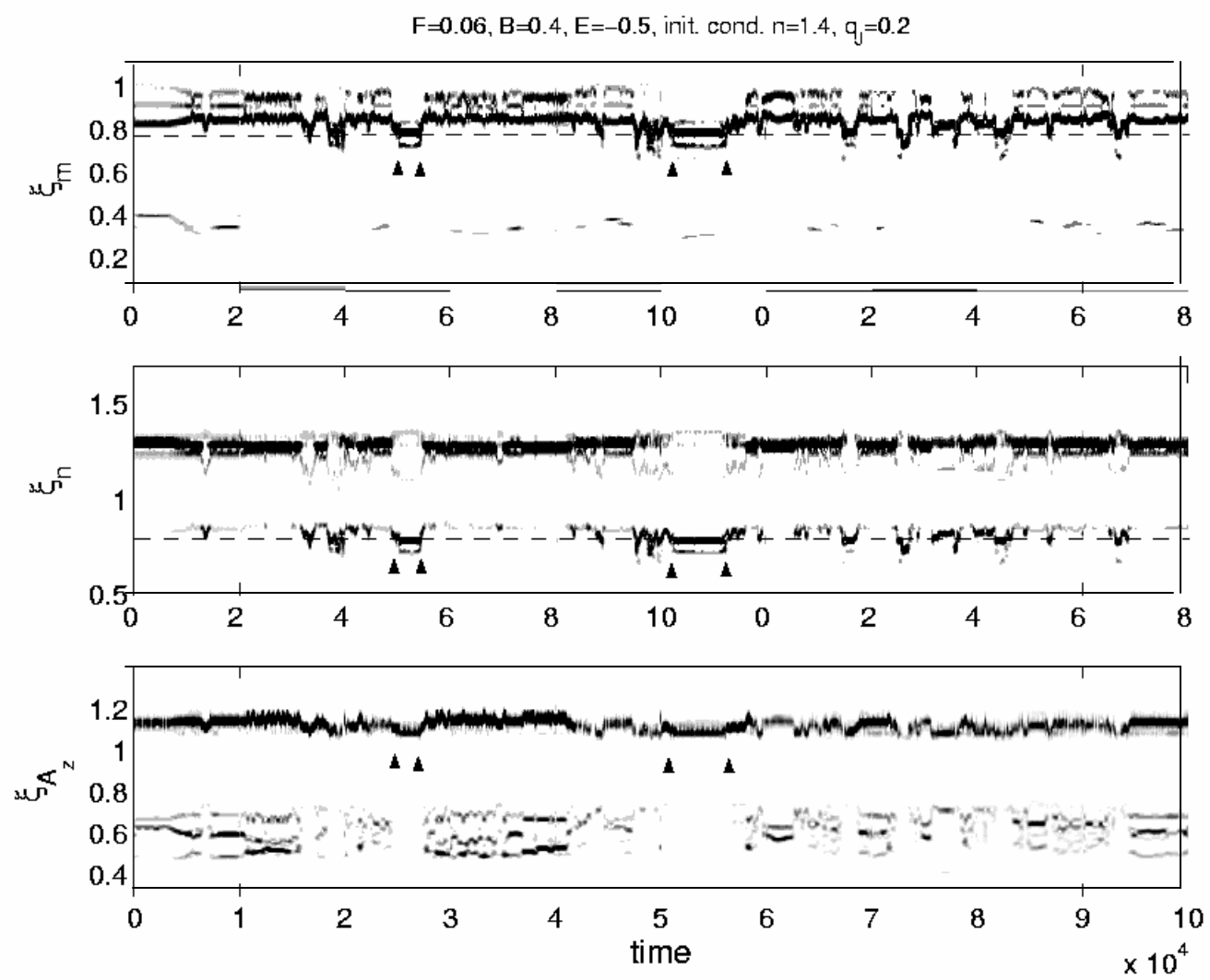

## Time-frequency decomposition

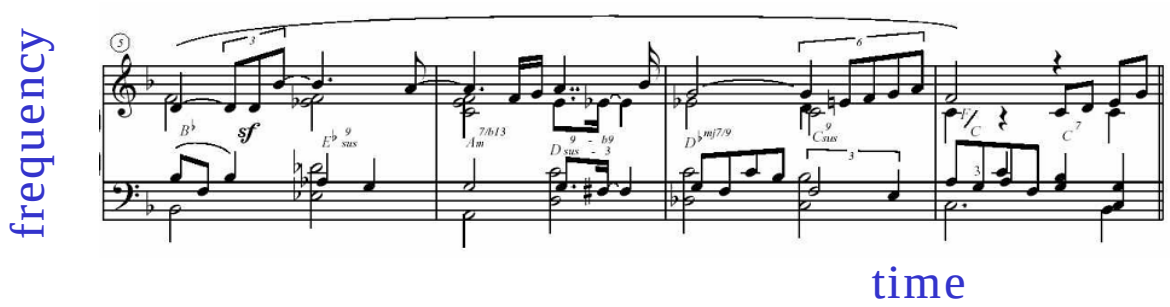


*Grossmann - Morlet wavelet transform*

Re( $\psi(t)$ )

$$\psi(t) = e^{i\eta t} e^{-t^2/2\sigma^2}$$

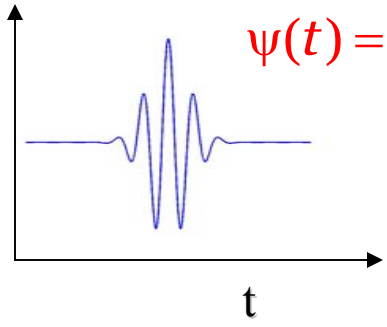


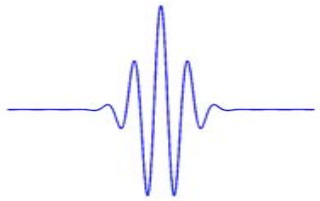

$$\Psi\left(\frac{t-u}{s}\right), \quad s>1$$

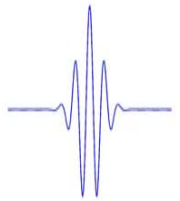

$$\Psi\left(\frac{t-u}{s}\right), \quad s<1$$

$$Wf(u,s) = \frac{1}{\sqrt{s}} \int_{-\infty}^{+\infty} f(t) \Psi^*\left(\frac{t-u}{s}\right) dt$$

$$\omega = \frac{\eta}{s}$$

Scalogram : $P_W(u,s) = \frac{1}{s} |Wf(u,s)|^2$

Reference: P. Goupillaud and A. Grossmann and J. Morlet , Geoexploration (1984 )